Policy Research Working Paper 9504

The Impact of Flooding on Urban Transit and Accessibility

A Case Study of Kinshasa

Yiyi He
Stephan Thies
Paolo Avner
Jun Rentschler

WORLD BANK GROUP
Global Facility for Disaster Reduction and Recovery
December 2020

Policy Research Working Paper 9504

Abstract

Transportation networks underpin socioeconomic development by enabling the movement of goods and people. However, little is known about how flooding disrupts transportation systems in urban areas in developing country cities, despite these natural disasters occurring frequently. This study documents the channels through which regular flooding in Kinshasa, the Democratic Republic of Congo, impacts transport services, commuters' ability to reach their jobs, and the associated economic opportunity costs from travel delays. This assessment is based on transit feed specification data sets collected specifically for this analysis under normal and flooded conditions. These data sets were combined with travel survey data containing travelers' socioeconomic attributes and trip parameters, as well as a high-resolution flood maps. The results show that (1) flood disruptions cause increases in public transit headways and transit re-routing, decreases in travel speeds, and thus travel time delays, which translate into substantial economic costs to local commuters; (2) accessibility to jobs decreases under flooded conditions, hindering the establishment of an integrated citywide labor market; (3) there are spatial clusters where some of the poorest commuters experience among the highest travel delays, highlighting socio-spatial equity aspects of floods; (4) certain road segments are critical for the transport network and should be prioritized for resilience measures; and (5) the estimated daily cost of flood disruption to commuters' trips in Kinshasa is $1,166,000. The findings of this assessment provide disaster mitigation guidance to the Office des Voiries et Drainage under the Ministry of Infrastructure, as well as strategic investment recommendations to the Ministry of Housing and Planning.

This paper is a product of the Global Facility for Disaster Reduction and Recovery. It is part of a larger effort by the World Bank to provide open access to its research and make a contribution to development policy discussions around the world. Policy Research Working Papers are also posted on the Web at http://www.worldbank.org/prwp. The authors may be contacted at yiyi_he@berkeley.edu, pavner@worldbank.org, and jrentschler@worldbank.org..

The Impact of Flooding on Urban Transit and Accessibility — A Case Study of Kinshasa

Yiyi He, Stephan Thies, Paolo Avner, Jun Rentschler

Keywords: flooding, multi-modal network model, travel disruption, infrastructure resilience, GTFS

JEL Codes: Q54, C63, R11, R14, R23

Acknowledgments: We would like to thank GoMetro for leading the public transport mapping, and in particular Bob Kabeya and Clayton Lane, as well as the enumerators that conducted these surveys. We thank Shohei Nakamura, Takaaki Masaki and Mervy Ever Viboudoulou Vilpoux for their help in accessing Kinshasa commuter and household surveys. We are grateful to Laurent Corroyer, Stephane Hallegatte and Kirsten Homman for their inputs and feedback throughout this project. We are also grateful to Catalina Ochoa for her review of an earlier draft of this paper and her thoughtful comments. This study was supported by the Global Facility for Disaster Risk Reduction and Recovery (GFDRR).

1 Introduction

Transportation networks provide critical socio-economic services at local and regional scales. However, demographic and economic growth, rapid urbanization, increasing infrastructure interdependency, and natural hazards – due to the worsening effects of climate change – are putting physical transportation systems under increasing pressure (Chen & Wang, 2019; Schreider et al., 2000). This is particularly evident in urban areas where transport networks are especially vulnerable to weather-related hazards (Pregnolato, Ford, Glenis, et al., 2017; Singh et al., 2018; Yin et al., 2016). Improving their resilience to natural hazards and extreme weather events has become a vital aspect of governing and managing an economically-viable and livable city (Pregnolato, Ford, Wilkinson, et al., 2017).

Flooding, especially flash flood events due to extreme precipitation, is the predominant cause of weather-related disruption to the transport sector (DfT, 2014). Floods reduce transportation network capacity, either directly through physical destruction rendering roads unusable or through floodwater accumulation on the road surface rendering the road impassable. Both cases could lead to severe localized traffic congestion that later propagates to regional levels (Mao et al., 2012; Rentschler et al., 2019). Kasmalkar et al., (2020) studied the impact of coastal flooding with respect to traffic disruption in the San Francisco Bay Area and showed that flooding would render road segments impassable and lead to significant delays in commuters' travel times. In some areas, the delay was more than double the average travel time within the region of study. These types of disruptions would cause significant socio-economic costs in the form of increased travel distances and times for commuters (B. Kim et al., 2018).

In the past decades, many studies have focused on understanding the economic impact of flooding on urban transportation networks using various types of methods, such as widely used input-output (I-O) models (T. J. Kim et al., 2002; Okuyama, 2007), the dynamic REMI TranSight model by Stewart (2006), or the spatial computable general equilibrium (SCGE) model by Tatano & Tsuchiya (2008). Many of these models require high-quality traffic data, abundant travel supply and demand information and accurate hazard mapping, making it difficult to apply these methods in developing country cities where such information is scarce. This study overcomes these challenges and conducts a comprehensive assessment of the effect of flooding on transportation networks in Kinshasa, Democratic Republic of the Congo (DRC). This assessment is made possible through the use of state of the art transportation modeling techniques and by combining three data sets: 1) An innovative General Transit Feed Specification (GTFS) data set collected for the purpose of this analysis under normal (dry) and flooded (wet) conditions, 2) a travel survey data set with travelers' socio-economic attributes and Origin-Destination (OD) information, as well as 3) a set of high-resolution global flood maps that capture both the extent and depth of pluvial and fluvial floods. This study provides insights into the following research questions: 1) How does flooding impact multiple modes of transportation in Kinshasa in terms of headways, travel speed, travel itinerary, public transit service frequency, etc.? 2) How does flooding impact job accessibility and commuting times for different income groups and what are the corresponding opportunity costs? 3) Which road segments should be prioritized for flood protection and mitigation plans in terms of network criticality and vulnerability to pluvial and fluvial flooding?

2 Characterizing the Case Study Area

Kinshasa, the capital of the DRC, is situated by the Congo River. Once a site of fishing and trading villages, Kinshasa is now a megacity with an estimated population of more than 14 million ("Kinshasa," 2020),

making it the largest city in DRC and the second-largest in Africa (World Bank, 2020). Approximately 320 miles (515km) from the mouth of the Congo River, Kinshasa belongs to the greater Congo Basin (Figure 1)- the world's second-largest river in terms of catchment area (3,687,000 kilometres^2) and annual average discharge (41,800 m^3s^{-1}) (O'Loughlin et al., 2020).

In the last few decades, studies have shown an increase in the likelihood of extreme events, such as intense rainfall due to climate change (IPCC, 2014; Kasmalkar et al., 2020). The complex hydrological processes at the Congo Basin are sensitive to these climatic changes, resulting in an increase in the frequency of pluvial and fluvial flooding, which could lead to serious disruptions in socio-economic networks (Tshimanga et al., 2016). In the past, Kinshasa has experienced multiple cases of flash floods resulting from extreme precipitation after prolonged dry spells. When compounded with other hazards, such as landslides and earthquakes, the consequences can be devastating. In January 2018, flooding and landslides induced by consecutive days of extreme precipitation struck nine communes of Kinshasa, affecting more than 15,700 people and claiming 51 lives (International Federation of Red Cross and Red Crescent Societies, 2018).

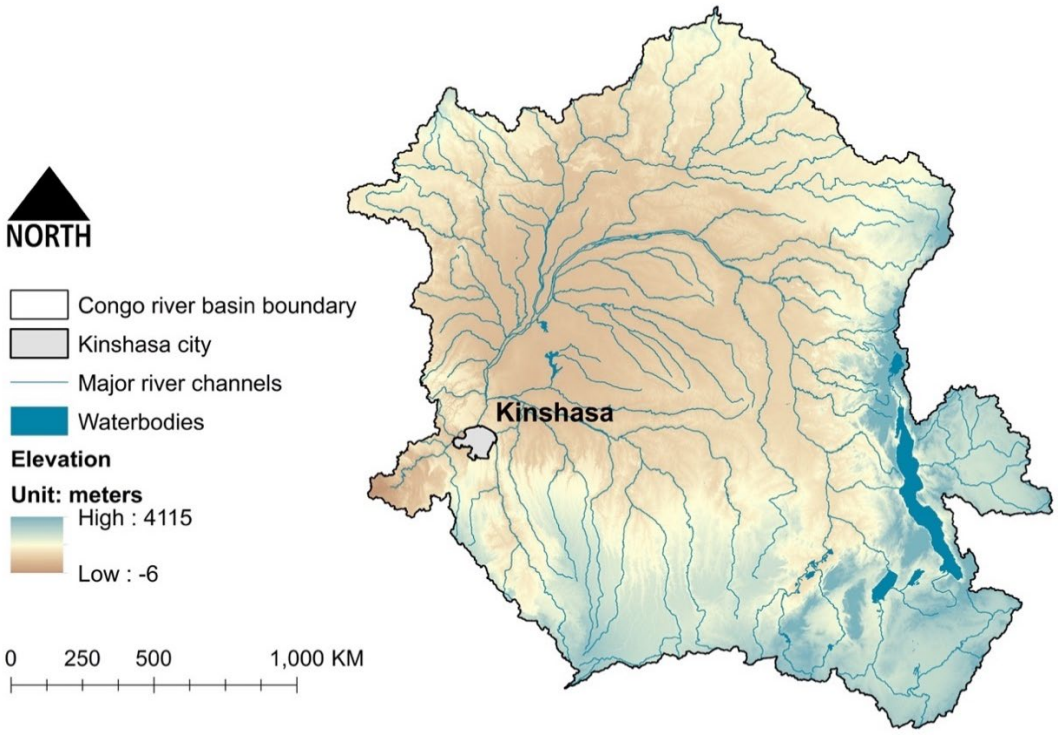

Figure 1: Hydrological network within the Congo River Basin and the location of the Kinshasa city.

3 Data and Preprocessing

3.1 Commuter Travel Survey

The Kinshasa Commuter Travel Survey (CTS), conducted by the Japan International Cooperation Agency (JICA, 2018), reports information on local commuting patterns as well as socio-economic attributes at both household (income/expenditure, number of vehicles, members, etc.) and individual (age/sex, work/school type and place, industrial category, income, vehicle availability, etc.) levels. The individuals and households are sampled based on Traffic Analysis Zones (TAZs), with sampling rates of about 100 to 400 samples for each TAZ (JICA, 2018).

Figure 2 shows a map of the TAZs in Kinshasa color-coded by population density in 2017 (people per square kilometer). The spatial extent of the TAZs covers not only the main city of Kinshasa with relatively high population density but also suburban towns and villages in the northeast within the city-province's administrative boundary. Figure 3 shows the travel connections in Kinshasa based on the commuters' reported trip origin and destination (OD) locations color-coded by commuters' income levels. It should be noted that approximately 40% of the trips do not have the exact spatial location of the ODs in the original CTS output data. A statistical model is used to provide estimations (see section 7).

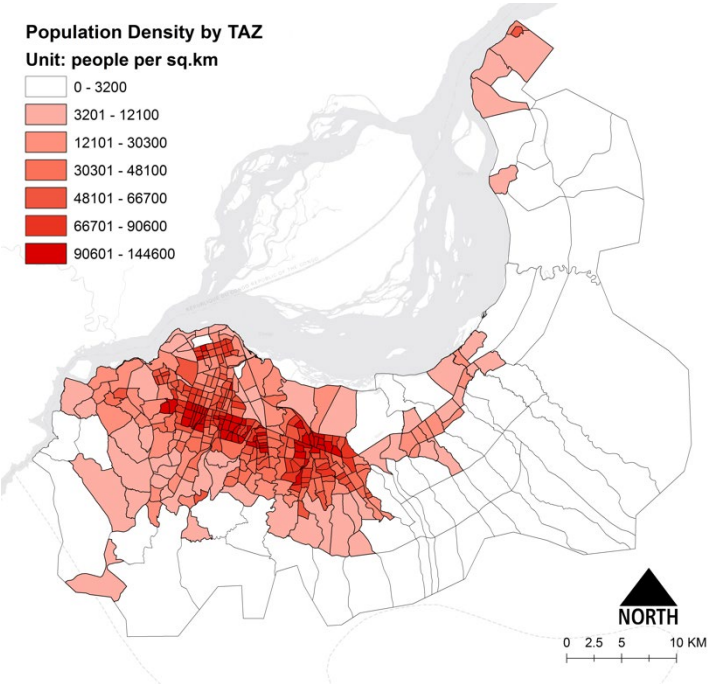

Figure 2: Population density (people per sq.km) by TAZ in Kinshasa (2017).

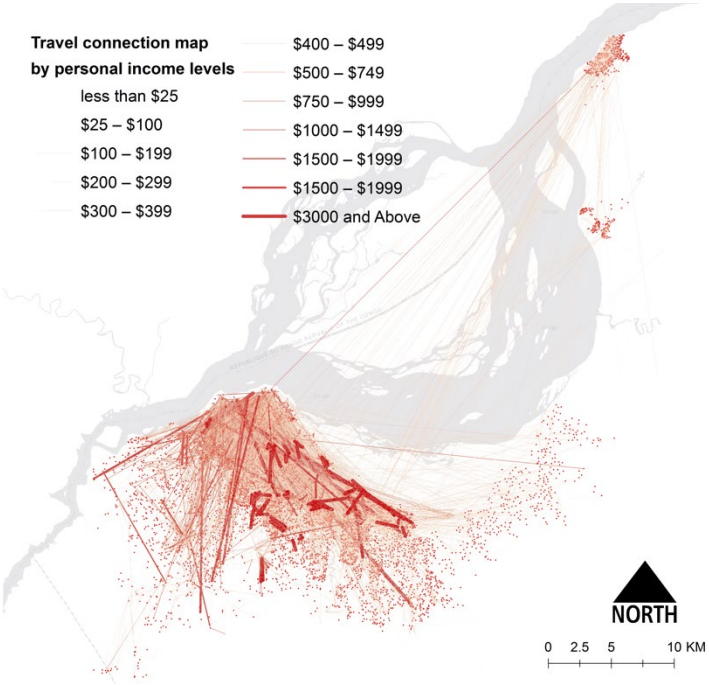

Figure 3: Travel connection map by personal monthly income levels in Kinshasa.

3.2 General Transit Feed Specification (GTFS) Public Transit Feed

GTFS, a data specification, allows public transit agencies to publish their transit data in a format that can be consumed by a wide variety of software applications. It includes a static component that contains schedule, fare, and geographic transit information and a real-time component that contains arrival predictions, vehicle positions, and service advisories (GTFS, 2020). It has been widely used in transportation operational research and network modeling in developed economies (Perrine et al., 2015; Wong, 2013). However, this data set is difficult to establish and maintain in developing economies due to various challenges: informal transit networks, unpredictable and low service quality, unavailability of publicized route maps, fare schedules or operating hours (Krambeck & Qu, 2015).

Static GTFS feeds were collected for the purpose of this study under normal (dry) and flooded (wet) conditions for five main types of public transportation[1]: Transco, Esprit de Mort, Esprit de Vie, Taxi Jaune, and Moto Taxi. Table 1 provides a detailed description of these public transportation modes. GTFS data collection under dry conditions was conducted over three weeks from January 30 to February 25, 2020; wet condition GTFS data were collected from March 5 to March 22, 2020 which coincides with one of the heights

[1] The data collection was conducted by GoMetro, a firm specializing in public transport data collection and planning solutions.

of Kinshasa's rainy season.[2] The average daily rainfall amount in March 2020 was approximately 190 millimeters which is greater than the 77th percentile of average daily rainfall between 1901 and 2016 (Figure 4). In addition, 28 out of 31 days in this month were rainy. The wet mapping exercise was conducted within 48 hours after heavy rains and flooding in Kinshasa. The routes were mapped using the GoMetro Pro mobile mapping application and this enables enumerators to collect data using GPS. For the data collection wave (dry and wet mapping), a total of 58 enumerators made over 200 public transit trips, recording number of trips per transport route, number of passengers per vehicle, revenue per vehicle, GPS location of all stops, vehicle travel distance, vehicle travel time, vehicle stop waiting time, vehicle headway,[3] etc. Details of GTFS feeds mapping under dry and wet conditions are provided in Table 2.

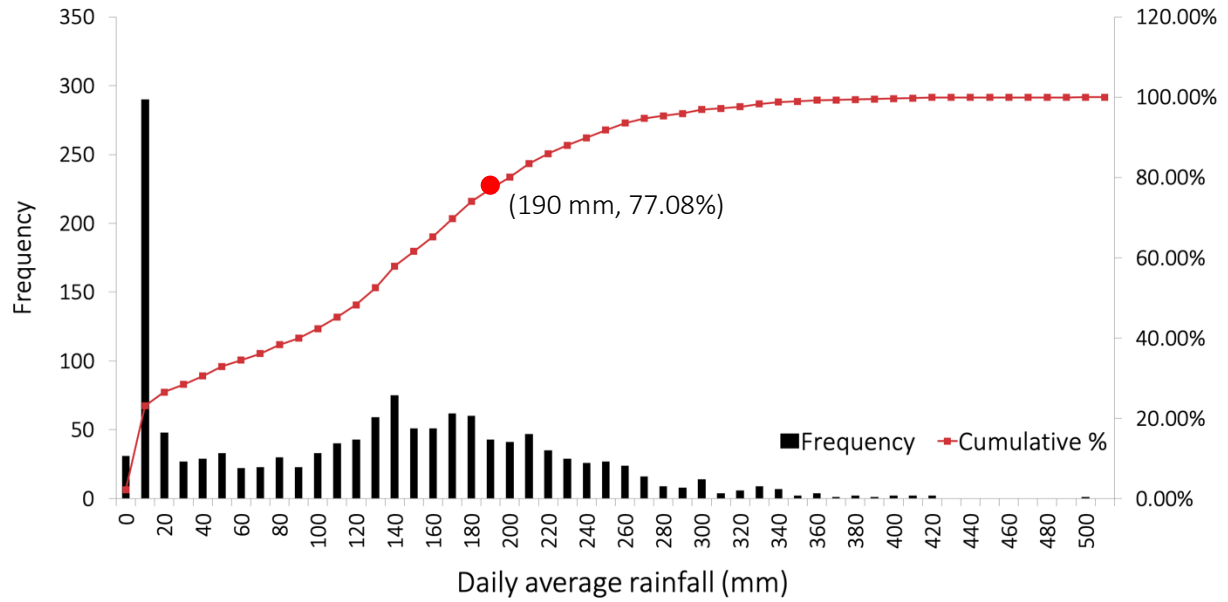

Figure 4: Histogram of aveage daily rainfall (mm) and corresponding cumulative distribution based on historical records from 1901 to 2016.

To the best of our knowledge, this dual-condition GTFS mapping has never been done before, making this effort the first of its kind. It should be noted that the wet GTFS mapping in Kinshasa covers approximately 28% of the transport lines surveyed under dry conditions.[4] The lack of overlap between dry and wet mapping prevents meaningful, unconditional comparisons of the summary statistics presented in Table 2. For example, for each transport mode, travel speeds under dry and wet conditions cannot be compared directly due to two reasons. First, only a share of the routes were surveyed during wet conditions, and second, even for routes surveyed under both dry and wet conditions, the itineraries were not necessarily the same. To overcome this issue we developed a matching method that is detailed in section 4.1.

[2] The other height of Kinshasa's rainy season is around November.

[3] The time between public transit departures from the same stop.

[4] With respect to the total number of routes, 72 % fewer routes were mapped under wet conditions than under dry conditions. Comparing the total length of the networks 59% fewer routes were mapped under wet conditions than under dry conditions.

Table 1: Details of five modes of public transportation operating in Kinshasa.

Transco	Esprit de Vie	Esprit de Mort	Taxi Jaune	Moto Taxi
The main public bus service in Kinshasa. In 2020, there are more than 40 bus routes with a total of 986 bus stops (Moovit, 2020).	Minibus taxis with a capacity of up to 22 seats.	Bigger taxis which are usually operated with Mercedes Benz 207 models for inter suburbs trips and long-distance travels within the city.	Cabs painted in yellow with a capacity of four passengers. They usually operate between neighboring suburbs and complete most of the first and last mile services within the city.	Informal moto taxi that provides connection to areas that are enclaved and not easily accessible due the condition of roads and congestion levels. In other instances, trips shorter than three kilometers are done using moto taxi as a first and last mile service.

Table 2: Summary details of GTFS trip mapping under dry and wet conditions.[5]

	Transco		Esprit de Mort		Esprit de Vie		Taxi Jaune		Moto Taxi	
	dry	***wet***	***dry***	***wet***	***dry***	***wet***	***dry***	***wet***	***dry***	***wet***
Number of routes	42	-	66	52	31	11	299	67	39	-
Number of stops	499	-	502	453	292	102	1945	392	97	-
Number of route segments	457	-	436	401	261	91	1646	325	58	-
Total network length (km)	623	-	725	615	355	130	2254	774	172	-
Mean route segment length (km)	1.36	-	1.66	1.53	1.36	1.43	1.37	2.38	2.97	-
Mean travel speed (km/h)	24.7	-	24.2	26.7	24.8	21.9	24.8	27.3	23.9	-
Median travel speed (km/h)	18.5	-	22.3	17.0	22.0	17.0	17.7	19.3	22.8	-
Max travel speed[6] (km/h)	178.3	-	101.6	99.0	96.2	106.6	148.2	89.6	80.5	-

3.3 Open Street Map (OSM) Road Network Data Set

In addition to the five public transportation networks, we also added the drive as well as the pedestrian network leveraging the Open Street Map data set to account for commuters who walk or drive to work. The OSMnx Python package was used to create topological graph structures for the drive and pedestrian network layers (Boeing, 2017). These two network layers were later integrated with the five public transport layers to create the final multi-modal network[7] model for Kinshasa.

[5] There are no GTFS records for Transco bus and Moto taxi mapping under flooded (wet) conditions.

[6] Unreasonably high travel speeds can occur due to small inaccuracies in the GTFS files, but are clear outliers. If two stop points along a route are very close (in reality or due to GPS inaccuracies) and a surveyor enters a travel time which is a few seconds off, resulting travel speeds might exceed 100 km/h, which is unreasonable in an urban public transport setting. In the entire data set there are fewer than 10 route segments (<0.3%) affected by such inaccuracies.

[7] The multi-modal network is created based on both the GTFS feed and OSM data set, which provide speed limits for every road segment. For the pedestrian network, we assume 4.5km/h travel speed.

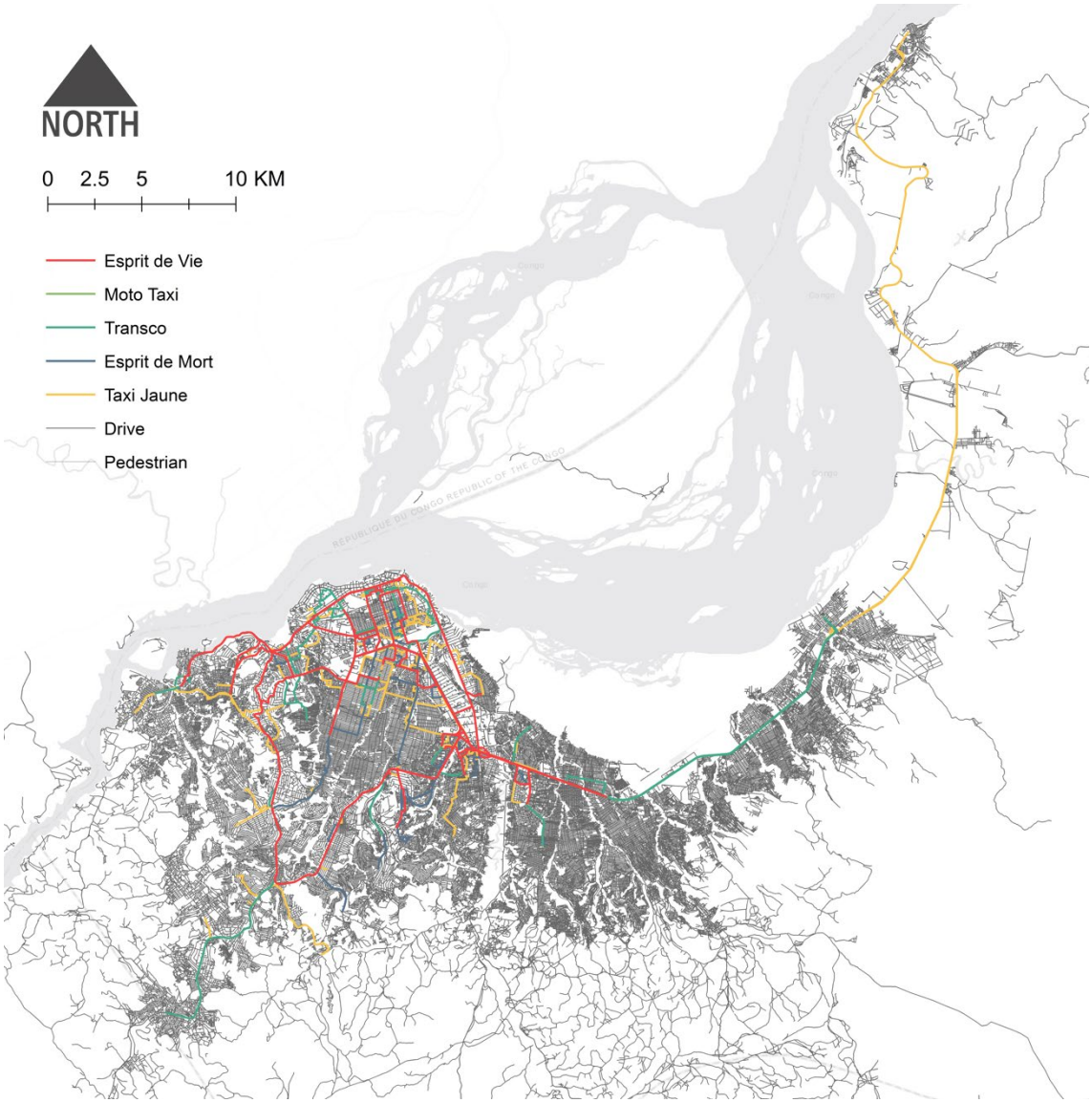

Figure 5: Seven transportation network layers in Kinshasa.

3.4 Fathom Flood Maps

Flood models are an integral tool for understanding and managing flood risks on transportation networks. In the past decades, increased computing power and precision of remote sensing data sets have led to the development of multiple global flood models (Bernhofen et al., 2018; Wood et al., 2011). Among them, the lastest flood map products from Fathom (A. Smith et al., 2015) are selected to provide flood depth and extent estimates in Kinshasa for the following reasons: 1) the map products from Fathom have relatively high spatial resolution (90 meters) which is sufficient for this study given the geographic extent of the Kinshasa city; 2) flood extent and depth estimates for both pluvial and fluvial floods under 10 return periods[8] are included in this data product; 3) it uses 2D hydrologic flood model which is more advanced in mapping flood plain and modeling dynamic water flows.

[8] Flood return periods of 5, 10, 20, 50, 75, 100, 200, 250, 500 and 1000 are included in the Fathom data product.

Pluvial and fluvial flood maps from the Fathom global flood model were first clipped to the bounding box[9] of the Kinshasa city and then mosaiced together using the maximum operator so that the maximum flood depth from both fluvial and pluvial flood estimates were preserved. Among the 10 different return periods that Fathom flood map products offer, the 10-year return period was used for our central analysis as it provides a good approximation of the impact of flash floods during the rainy season in Kinshasa. Given historical rainfall records from 1901 to 2016 (Figure 4), the frequency of the actual flood events that occurred during the wet transit mapping period is likely greater than 1/10. However, selecting the 10-year Fathom flood map in our analysis yields a more conservative estimate of the travel disruptions when lacking detailed information of hourly rainfall intensity. In practice we therefore attribute transit disruption impacts (speed reductions, reduced frequencies) from annual, limited intensity events to less frequent, higher intensity flood episodes. This method will avoid the overestimation of transport disruption impacts from floods and will yield robust lower bound estimations of the costs of floods on commuting. We also run the analyses documented in this study for 50, 100, 500 and 1000 flood return periods which allows us to compute an annualized estimate of the costs of floods from commuting delays (see section 4.4 for more details).

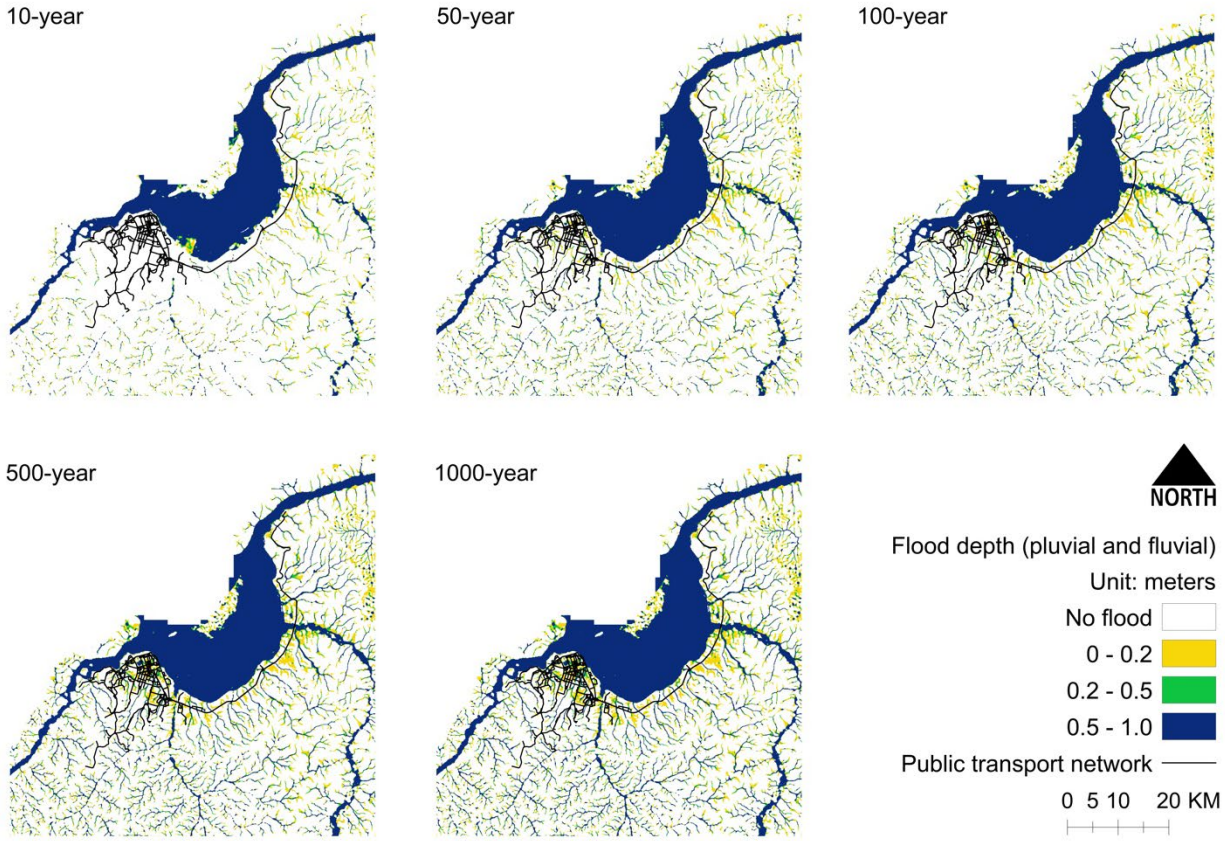

Figure 6: Combined flood maps with maximum flood depth from pluvial and fluvial flooding for five flood return periods: 10-year, 50-year, 100-year, 500-year and 1000-year.

[9] The bounding box around the Kinshasa city can be defined using the geographic coordinates below: -3.917dd, -4.624dd, 15.071dd, 15.716dd.

4 Empirical Analysis and Results

The goal of this study is to understand how pluvial and fluvial floods impact the transportation system in Kinshasa with respect to transit operations, job accessibility, road segment criticality, and economic loss (due to travel delay). We achieve this goal by collecting useful information on transportation network topology, commuter travel patterns, commuter socio-economic status, pluvial and fluvial flood maps from the sources mentioned above. Figure 7 shows a simplified workflow of this study from data collection to modeling and simulation to results. The following subsections will explain the details of the analysis and modeling process with corresponding results.

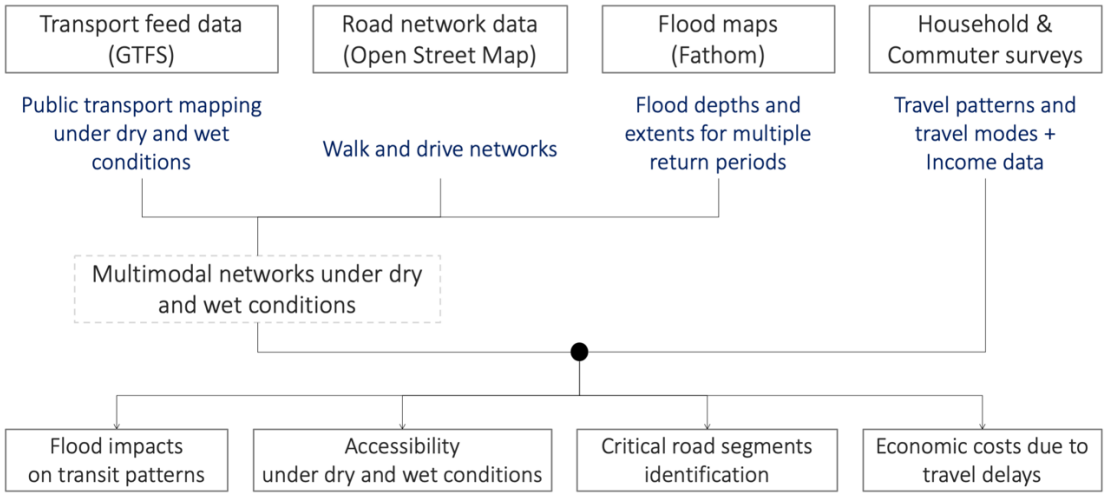

Figure 7: Overall project workflow from data collection, processing and analysis.

4.1 Flood Impacts on Transit Network

To understand the impact of flooding on public transit, we compared the GTFS transit feed mapped under dry and wet conditions and evaluated changes in headways, blockages of roads and rerouting, and travel speeds. The Transco bus network was observed as not operating under wet conditions when the survey took place. The Moto Taxi network was surveyed during dry conditions, in specific neighborhoods where direct access to other transit modes was not available. But this partial survey was not reproduced under wet conditions. The empirical analysis was therefore restricted to the Esprit de Mort, Esprit de Vie, and Taxi Jaune modes of transport. A special emphasis lies on the effects of flooding on travel speeds, for which an innovative matching method was developed allowing the robust estimation of changes in travel speeds while minimizing the potential impact of confounding factors (see section 4.1.3). The results from this empirical analysis section subsequently fed into the simulation study that was used to estimate the economic cost of flooding in Kinshasa.

4.1.1 Changes in headways

In the static GTFS feeds, surveyors reported a headway for each public transport route. As public transport is mostly informal in Kinshasa and no official timetable exists, these headways were observed by the surveyors and provide the frequency at which a bus, mini-bus, or taxi operates. All transport networks which were mapped under dry and wet conditions experience an increase in headways during the rainy season (Table 3). The informal minibuses-Esprit de Mort operate on average every 44 minutes under wet conditions compared to every 31 minutes under dry conditions. In addition, the Esprit de Vie and the Taxi Jaune operate 10 minutes and 9 minutes less frequently during wet conditions. An explanation for the increase in headways

is that transport vehicles operate less frequently to conserve material, avoid wear and tear, and prevent accidents due to wet and muddy roads. Additionally, full two-way cycles might take longer during wet conditions. This implies that more vehicles are needed per route to uphold dry condition headways. If the number of available vehicles is limited, headways will increase.

Table 3: Changes in headways due to rain and flooding by transport mode and time of the day.

	Esprit de Mort			**Esprit de Vie**			**Taxi Jaune**		
	Dry	Wet	Δ	Dry	Wet	Δ	Dry	Wet	Δ
Mean headway (min)	31	44	13	34	46	10	12	21	9
By time of the day:									
05:00 - 10:00	18	32	14	23	37	14	7	16	9
10:00 - 15:00	43	47	4	43	47	4	17	26	9
15:00 - 19:00	33	57	24	34	57	14	12	21	9

Notes: The mean headway was calculated across all transport routes of the respective transport mode, conditional on the respective time of the day.

4.1.2 Blockages of roads and changes in routes

When comparing inbound and outbound routes from dry and wet mapping, we found changes in travel trajectories. As each route was mapped only once, it is hard to identify a certain itinerary which could function as a baseline scenario when comparing routes under dry vs. wet conditions. The result of the comparison suggested that original routes were rerouted due to flooding. It is difficult, however, to pinpoint the exact reason for rerouting since both floods and other confounding factors such as road closures, traffic accidents or regulartory restributions can all result in changes in original routes.

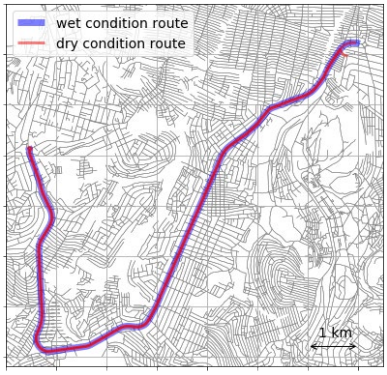

A) Esprit de Vie, Rond Point Ngaba - UPN

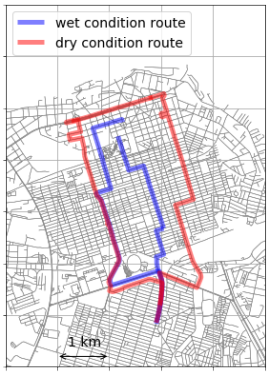

B) Taxi Jaune, Gombe Centre Ville - Victoire

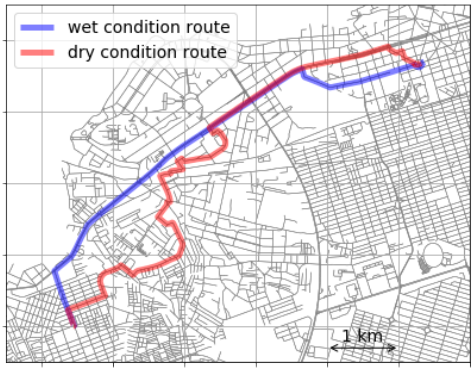

C) Esprit de Mort, Gombe Centre Ville - DGC

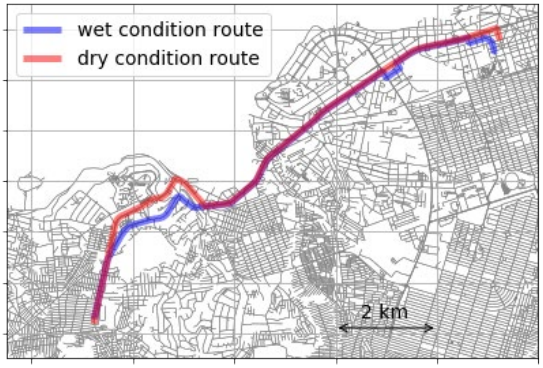

D) Taxi Jaune, Gombe Centre Ville - Velodrome

Figure 8: Four cases of rerouting under dry and wet conditions.

4.1.3 Changes in travel speeds

Unconditional comparisons of mean travel speeds as presented in Table 2 suggest that speeds of some public transport modes increase during rain and floods. However this unexpected result is skewed for two reasons: (1) in contrast to the dry network, only a fraction of the wet network was surveyed so that different route samples prevent from direct comparisons, and (2) wet network routes that were surveyed substantially differ from dry network routes. They had different origin and destination coordinates and took different trajectories. In fact, when locating OD points, GoMetro reported that only 30 out of 130 wet network routes can be matched with a corresponding dry network route. Even on the matched routes, trajectories might differ substantially (for examples of routes considered as matched see Figure 8). For these reasons, we could not rely on unconditional comparisons of average travel speeds on transit networks to understand the impact of heavy rain on travel speeds.

In this section, we estimated speed effects only for the overlapping parts of the surveyed wet and dry networks and net of rerouting. We matched and compared travel speeds under dry and wet conditions locally (within a 100-meter radius) and conditional on the mode of transport.[10] Relying on a bootstrap approach (Efron & Tibshirani, 1993), we then showed that differences in travel speeds pointed in the expected direction and are significant. They were also larger on route segments situated in flood-prone areas, though the effect was estimated with low precision. Therefore, in the next section, we rely on dry route trajectories to build a representative wet network, but adjust travel speeds to wet conditions using estimates provided here. This was an important part of the analysis as few papers previously inferred the impact of flooding and rain on travel speeds in developing countries such as the DRC. Former research focused on developed countries where an abundance of public transit data facilitates the estimation. Further, the estimation of travel speeds under wet conditions is crucial in our simulation study that provides accessibility and economic loss estimates due to floods (sections 4.2 and 4.4).

Matching procedure

The following lays out in detail the different steps involved in the matching procedure, illustrated in Figure 9. It also explains how significance tests were constructed, relying on the bootstrap methodology.

We denote the set of all route segments: $R = \{R^{dry}, R^{wet}\}$. A route segment r is defined as part of a route extending from one stop point to the next. Data on route segments can directly be obtained from the GTFS feeds. First, each route segment is transformed into a set of support points by resampling points every d meters along the route (Figure 9, panel B). Denote the resulting set of support points P_r. Each point $r_i \in P_r$ has coordinates s_{r_i} and inhabits all other attributes from route segment r. Hence the assumed travel speed at point r_i, denoted v_{r_i}, is identical to the speed on route segment r, denoted v_r.[11]

[10] In robustness checks we further control for the time of the day but obtain similar results. The results are available on request.

[11] This implies that we do not correct for effects of acceleration and deceleration between two stops. We do not have information available to compute such a correction. Further, since travel speeds on route segments are usually low (around 25 km/h, see Table 2), we expect acceleration and deceleration effects to be negligible for our analysis.

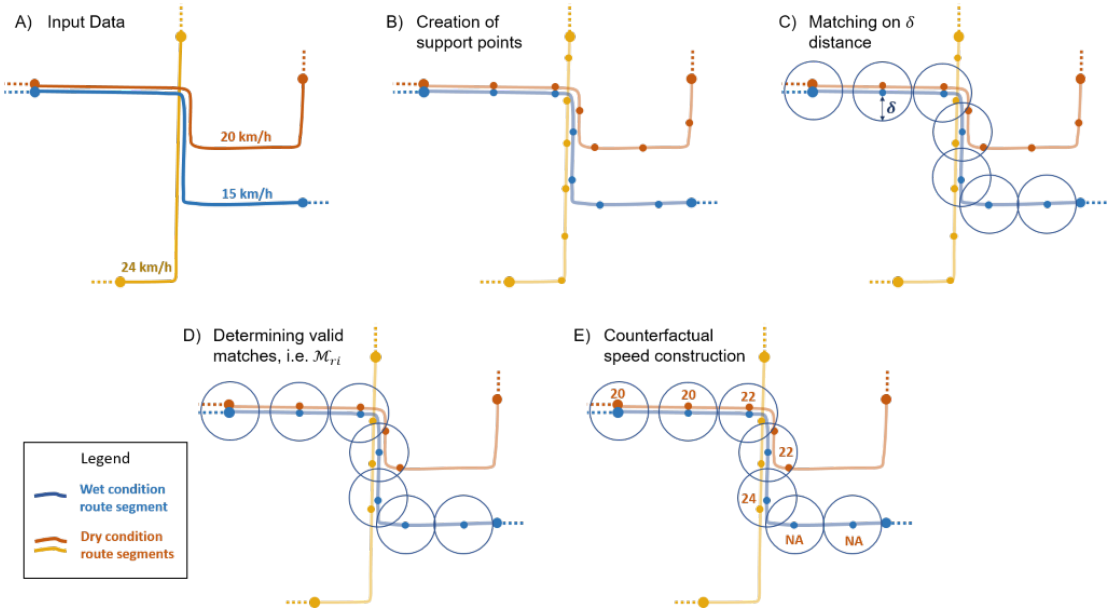

Figure 9: Illustration of the matching process.

In a next step, a counterfactual dry condition speed $\tilde{v}_{r_i}$ is constructed for each point that belongs to a route segment mapped under wet conditions (Figure 9, panels C-E). The counterfactual speed is the average speed of all dry condition routes that have support points within a δ distance of r_i:

$$\tilde{v}_{r_i} = \begin{cases} \frac{1}{M_{r_i}} \sum_{k \in M_{r_i}} v_k, & if \ \left|M_{r_i}\right| > 0 \\ NA \quad , & if \ \left|M_{r_i}\right| = 0 \end{cases}$$

Here, M_{r_i} is the matching set containing the indices of all dry routes passing through a δ neighborhood of r_i

$$M_{r_i} = \left\{ q \in R^{dry} : \text{distance}\left(s_{r_i}, s_{q_j}\right) \leq \delta \text{ for at least one } j \in P_q \right\}.$$

This matching procedure resembles coarsened exact matching as we do not require s_{r_i} and s_{r_j} to agree, but only require s_{q_j} to lie in the "coarsened", δ neighborhood of s_{r_i}.

One can then calculate the average effect of flooding on travel speeds for route r, denoted Δv_r, by averaging the differences of the actual speed under wet conditions and the counterfactual dry condition speeds at all support points r_i for which a counterfactual observation is available:

$$\Delta v_r = \frac{1}{|\mathcal{T}_r|}, \quad \text{where} \quad \mathcal{T}_r = \{ i \in P_r : \tilde{v}_{r_i} \neq NA \}$$

The network-level impact of flooding on travel speeds can finally be calculated as:

$$\Delta v = \frac{1}{\sum_{r \in R^{wet}} |\mathcal{T}_r|} \sum_{r \in R^{wet}} \sum_{i \in \mathcal{T}_r} \left(v_{r_i} - \tilde{v}_{r_i} \right)$$

As support points are equally spaced, this methodology inherently weights for route segment lengths. A route which is two times longer than another route will have twice as many support points.

In the example from Figure 9 the speed on the wet route segment is 15 km/h and the speeds on two neighboring dry route segments are 20 and 24 km/h. As the routes run only partly in parallel, the local matching would yield the following estimated speed effect in this example:

$$\Delta v_r = 15 - \frac{1}{5}(20 + 20 + 22 + 22 + 24) = -6.6 \text{ [km/h]}$$

The two central parameters in the matching procedure are the resampling distance d and the matching distance δ. The resampling distance d determines how many support points are generated. With decreasing d the number of support points increases which makes results more precise. But it also increases the computational costs of the matching procedure. When the matching distance δ is increased counterfactual dry speeds can be calculated for a larger share of support points. But at the same time the validity of the matches might suffer. For all results presented in the following a resampling distance d and a matching distance δ of 100 meters were chosen, finding a trade-off between computational costs and matching accuracy.

Bootstrap significance tests

Using the matching method outlined above, an estimated speed difference can be attributed to most route segments mapped under wet conditions (see Table 4 for matching percentages by network type). To test whether the speed differences inferred are also significant, the bootstrap method was used. Under the null hypothesis, speeds under dry and wet conditions are the same. Under the alternative hypothesis, speeds under wet conditions are smaller than speeds under dry conditions:

$$H_0: \Delta v = 0 \quad vs. \quad H_1: \Delta v < 0$$

We bootstrap the distribution of Δv under the null hypothesis by randomly assigning the dry or wet attribute to route segments. This corresponds to reshuffling R^{wet} and R^{dry} such that route segments which were originally element in R^{wet} (or R^{dry}) can be reassigned to either R^{wet} or R^{dry} since this assignment shouldn't matter under the null hypothesis. For each bootstrap iteration b the assignment is reshuffled and $\Delta v^{(b)}$ is calculated. Out of B bootstrap iterations one can then obtain an estimated p-value of the outlined test as

$$p_{boot} = \frac{\sum_{b=1}^{B} I\left(\Delta v < \Delta v^{(b)}\right) + 1}{B + 1}$$

Estimation of heterogeneous effects for flood prone areas

After speed differences were estimated for each route $r \in R^{wet}$, it was analyzed whether routes that are likely to be flooded during the rainy season show larger speed reductions than routes that are unlikely to be flooded. Similarly, to a diff-in-diff-in-diff (DDD) method, Δv_r was regressed on a dummy, indicating whether the flood depth in a 10-year flood would be positive:

$$\Delta v_r = \beta_0 + \beta_1 I(FD_r > 0) + \epsilon_r$$

Here, FD_r is the maximum flood depth on route r in a 10-year flood as indicated through the Fathom flood maps, β_0 is the average speed difference on routes that are unlikely to be flooded and β_1 is the additional speed difference on routes likely to be flooded. As before p-values for β_0 and β_1 were calculated using the bootstrap methodology, allowing for potential correlation within the error term ϵ_r.

Results

Results of the matching procedure outlined previously are presented in Table 4. They indicate that travel speeds of different public transport modes are lower during wet conditions than during dry conditions. The

estimated speed differences also differ substantially from an unconditional comparison of speeds as presented in Table 2, emphasizing the importance of a local comparison.

The speed reduction is most pronounced and significant for the Esprit de Mort transport network, which operates under wet conditions on average with speeds about 4 km/h slower than under dry conditions. For the Esprit de Vie and the Taxi Jaune network average speeds are estimated to lie about 2 km/h and 0.5 km/h below dry condition speeds respectively, but effects are not significant.

Considering the characteristics of the three different transport modes the estimated effects appear reasonable: The Esprit de Mort transport network is provided through old vehicles that are most likely to be affected through rain, mud, and wet conditions. On the Esprit de Vie network more modern mini-buses are operational. Taxi Jaune is the most flexible type of public transport infrastructure in Kinshasa and it is likely that the small vehicles can circumvent traffic jams due to flooding and easily reroute, hence obtaining speeds similar to dry conditions.

Additional results from the DDD regressions suggest that travel speeds are more affected on route segments that are more likely to be flooded. When considering for example the Esprit de Mort network under wet conditions, average travel speeds are about 3.7 km/h below dry condition speeds on all route segments outside the 10-year flood plain. Within the 10-year-flood plain, the speed reduction is more pronounced, and speeds are on average an additional 6.1, i.e. 9.8 km/h in total, lower than during dry conditions. However, this effect cannot be estimated with sufficient precision to be significant, most likely due to the small sample size: only 5.5% of the mapped Esprit de Mort network lie within the 10-year flood plain.

Table 4: Effects of rain and wet conditions on travel speeds by network type.

	Esprit de Mort		**Esprit de Vie**		**Taxi Jaune**	
	Estimate	p-value	Estimate	p-value	Estimate	p-value
Speed difference [km/h]						
Mean	-3.892	0.004	-1.667	0.271	-0.574	0.315
Median[12]	-3.197	0.022	-1.985	0.192	-1.573	0.192
DDD estimates using 10-year return period flood map						
% wet network within flood plain	5.50%		1.10%		9.23%	
β_0 (baseline speed reduction)	-3.700	0.004	-1.652	0.234	-0.812	0.299
β_1 (additional effect in flood plain)	-6.136	0.248	-2.400	0.657	0.987	0.657
Route segments wet	401 (615 km)		91 (130 km)		325 (774 km)	
Route segments dry	436 (725 km)		261 (354 km)		1646 (2254 km)	
Percentage wet network matched	76.30%		80.86%		96.04%	
Notes: All p-values are based on 500 bootstrap samples						

4.2 Accessibility

In this study, we measure workers' accessibility to jobs, and how it is threatened by urban flooding. The first step to accessibility calculation is understanding flood exposure levels on the road network, an important step to flood risk evaluation (Hall et al., 2003; Pregnolato, Ford, Wilkinson, et al., 2017). We quantified network exposure to the 10-year flood by spatially overlaying the maximum mosaic of pluvial and fluvial flood maps with the multi-modal transportation network. As a result, we were able to calculate the inundation level for each road segment in the study area. Next, we adjusted travel speeds on road segments based on inundation depth. After engaging with local transportation planning officials in Kinshasa, we came to the understanding that most vehicles that operate on the road networks in Kinshasa were relatively small and

[12] Median speed differences are calculated through the matching methodology conceptually in the same manner as mean differences, but by replacing in the calculation of Δv averages through median operators.

old models with exhaust pipes approximately 20 cm above the road surface. This means that when the flood water accumulates to 20 cm on roads, most vehicles would not be able to properly function. Among the 67,752 road segments in our study area, 802 had flood inundation depth greater than 0.2 cm.

Next, we evaluated the impact of flooding on transport accessibility in Kinshasa by comparing the difference in travel time for commuters to reach their jobs. Generally speaking, the disturbance mechanism of floods on transportation network includes the following: 1) changes in headways, 2) road closure or rerouting, and 3) reduction in travel speed. These disturbance patterns are considered interdependent i.e. they can affect each other and the compounding effect of a combination of these patterns is greater than the sum. For example, reductions in travel speeds and blockages of streets due to flooding can lead to rerouting. Rerouting might allow higher travel speeds on alternative routes but can also lead to congestion. In turn, the overall impacts of flooding and rain on the public transport network are uncertain.

We carefully examined the impact of flooding on each disturbance pattern and 'perturbed' the original multi-modal network to create a network model that is able to capture all the changes in headways, road closure and travel speed reduction under a 10-year flood scenario. As only a fraction of the network under wet conditions was surveyed and we could not distinguish unsurveyed routes from routes non-operational due to flooding, we relied on the dry transport network to obtain a representative wet network. In particular, we obtained the wet network used for our accessibility simulations through the following modifications of the dry network:

1) We removed all Transco bus connections, as Transco busses were observed to be non-operational during heavy rain and flood.
2) We adjusted headways for each route conditional on network type as reported in section 4.1.1.
3) We reduced travel speeds on each route conditional on network type using the mean travel speed effects quantified in section 4.1.3: 4 km/h and 2 km/h speed reduction for Esprit de Mort and Esprit de Vie respectively.
4) We removed all route segments that are inundated in a 10-year flood

Building on the resulting wet network, we then ran travel simulations for a total of 8,866 commuters[13] in Kinshasa using the origin and destination location information provided in the JICA commuter travel survey under both dry and wet conditions for five flood return periods.

The left panel of Figure 10 shows the results of travel time simulations for 8,866 daily commuter trips under dry conditions. On average, the estimated daily commute time from home to work is 43.25 minutes. The right panel of Figure 10 shows the results from hot spot analysis of the travel time estimations with blue points showing clusters of low values and red points showing clusters of high values. We observe clusters of commuters who live in the suburban neighborhoods take longer to travel to work, whereas commuters who live in areas near the center of Kinshasa city take shorter time. Figure 11 compares the results from the travel time hot spot analysis with commuter personal income hot spots and highlights areas where these plots show diverging results. The southeastern and northeastern suburban areas show clusters of low-income values yet high travel time while the northern region near the Congo river show opposite patterns. This reveals socio-spatial equity issues, as certain low-income areas are systematically disadvantaged in terms of

[13] The 8,866 commuters are a subset of the people who were surveyed who declared their travel origin and destination to work.

job accessibility and economic opportunities. The left panel of Figure 12 shows the average travel delay results aggregated to the TAZs and the right panel shows the respective hot spot analysis outputs. The maps show that commuters who live in the southern regions of the city namely Kimvula, Ndjili kilambo, Kimbariseke etc. experience longer delays in travel time to their jobs whereas commuters who live in N'sele and Maluku experience shorter delays. The hot spot analysis reveals a more granular pattern in the spatial distribution of travel delays and provides a baseline for socio-spatial equity analysis.

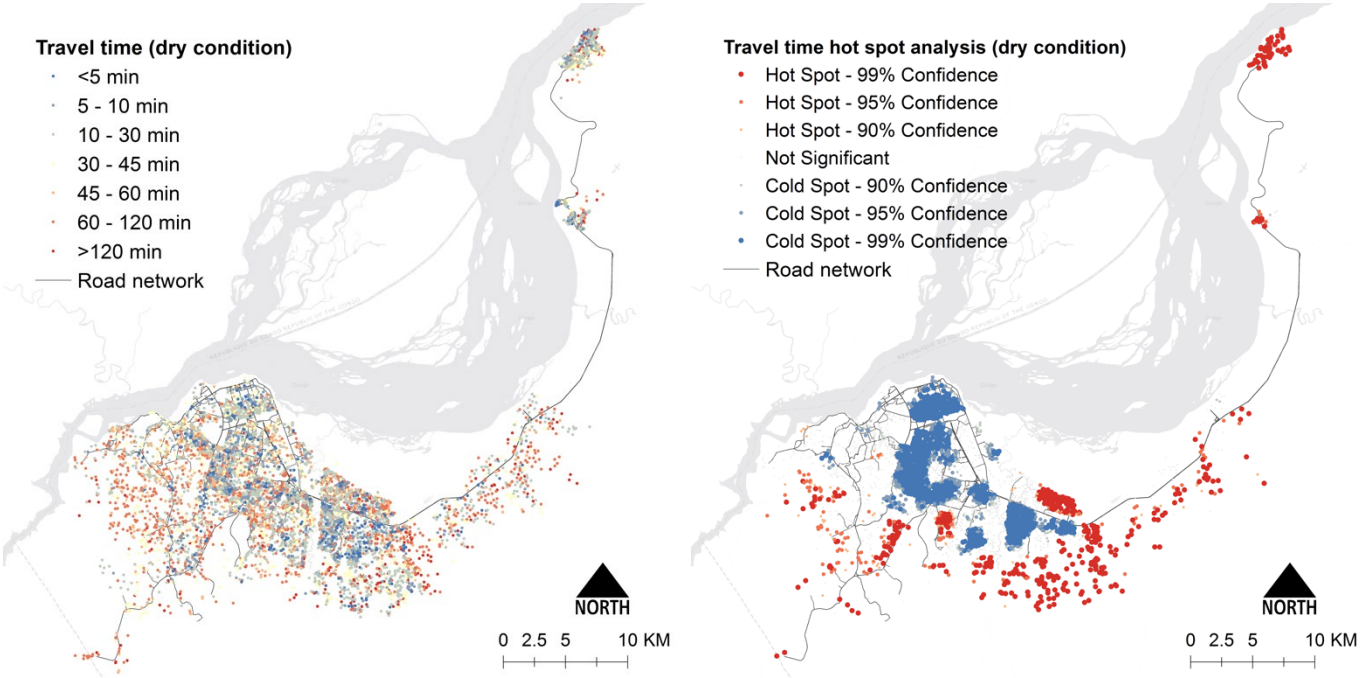

Figure 10: Map of commuters' travel time under dry scenario (left) and respective hot spot analysis output.

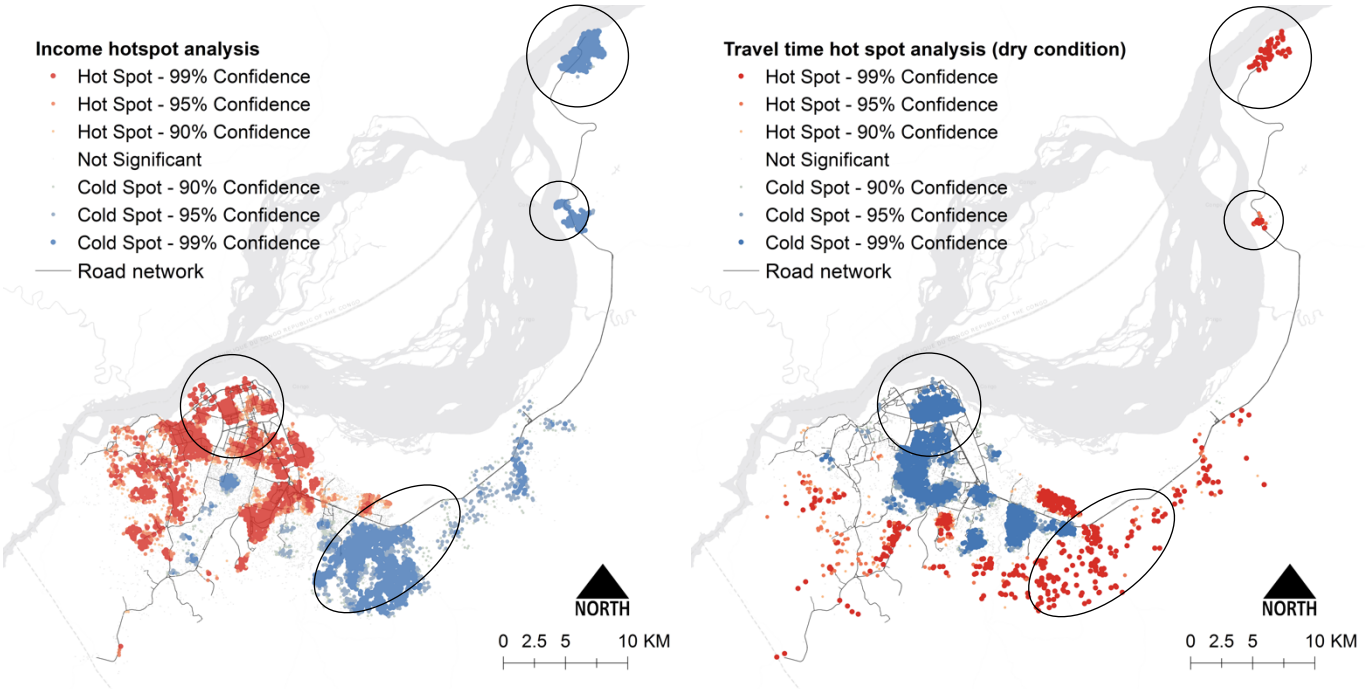

Figure 11: Hot spot analysis result for commuter income and travel time under dry conditions.

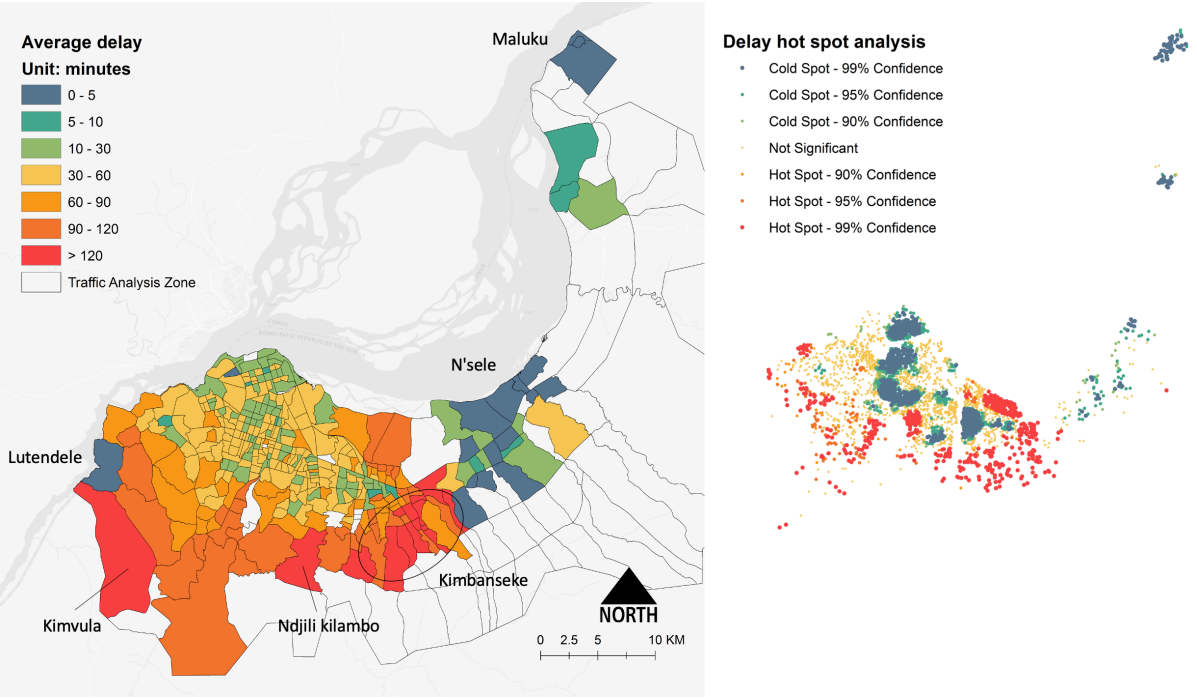

Figure 12: Map of average travel delay aggregated to Traffic Analysis Zones (TAZs) (left panel) and hot spot analysis on travel delay (right panel)

Using the TAZs as basic analysis units, we calculated one-hour accessibility for each TAZ using three types of transit networks: walking network, driving network, public transit network (with mean transit waiting time assumption).[14] We use TAZ polygon centroids as origins and simulated traveling time from each centroid to other centroids using the three transit networks under both dry and wet conditions. We measured one-hour accessibility for each TAZ and compared the change in the share of accessible jobs. Figure 13 shows boxplots of this change for each transportation network. On average, the loss in the share of jobs that can be reached within one hour is 0.1% for the walking network,[15] 10.9% for the drive network, 5.0% for public transit network. Due to the fact that the walking network has relatively high road density, i.e. the total length of roads per unit area, the impact of flooding on job accessibility with the walking network is comparatively small. We observe many extreme values for the drive network with 92.7% as the maximum loss of job accessibility. This might be caused by flood disruption on critical road segments which commuters depend upon to access job locations. Figure 14 shows the spatial distribution of the percentage loss of job accessibility under the 10-year flood scenario. In general, the TAZs that experience higher loss of job accessibility are concentrated along the Congo riverside, heart of the Kinshasa city. These areas overlap with TAZs that have a relatively high population density (Figure 14-D). The spatial distribution of loss of job access for the drive network shows a unique pattern with a larger loss of job access around suburban TAZs and minimal loss in the city center. This is potentially caused by uneven network density distribution of the drive network in Kinshasa. The drive network density in the city center is significantly greater than that in the suburbs with more redundancy. Even when some of the road segments are flooded, it is relatively easier to find an equally efficient alternative route in areas with higher network density. A summary of the

[14] We performed the same analysis for public transit networks with minimum and maximum waiting times as well and on average the loss of share of job increases by 2.2% and 3.7% respectively.

[15] Due to floodwater accumulation on roads, some parts of the walking network become impassable to pedestrians. In such cases, pedestrians often need to take another route (often longer in distance) to get to their destinations.

comparison between averaged one-hour job accessibility share under dry and wet conditions can be found in Table 5.

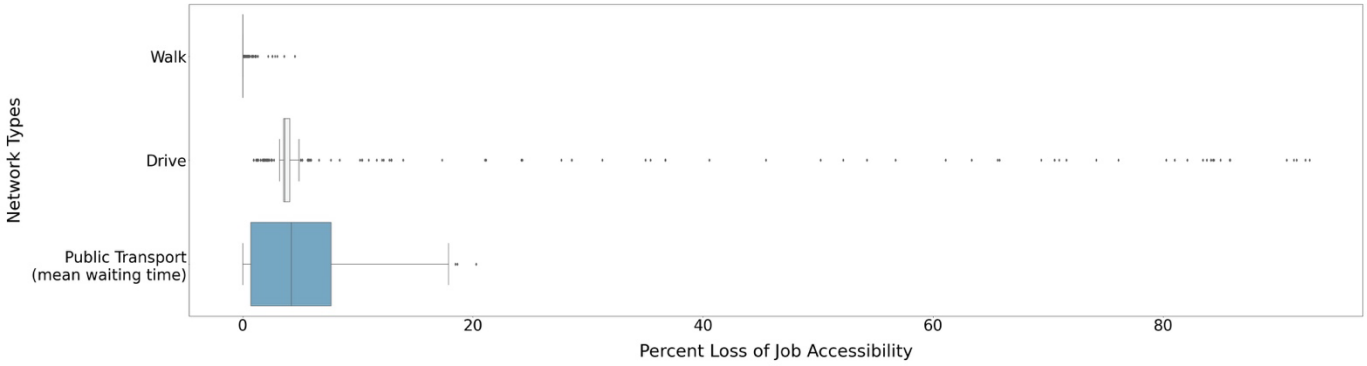

Figure 13: Changes in accessibility to share of jobs under dry and wet conditions.

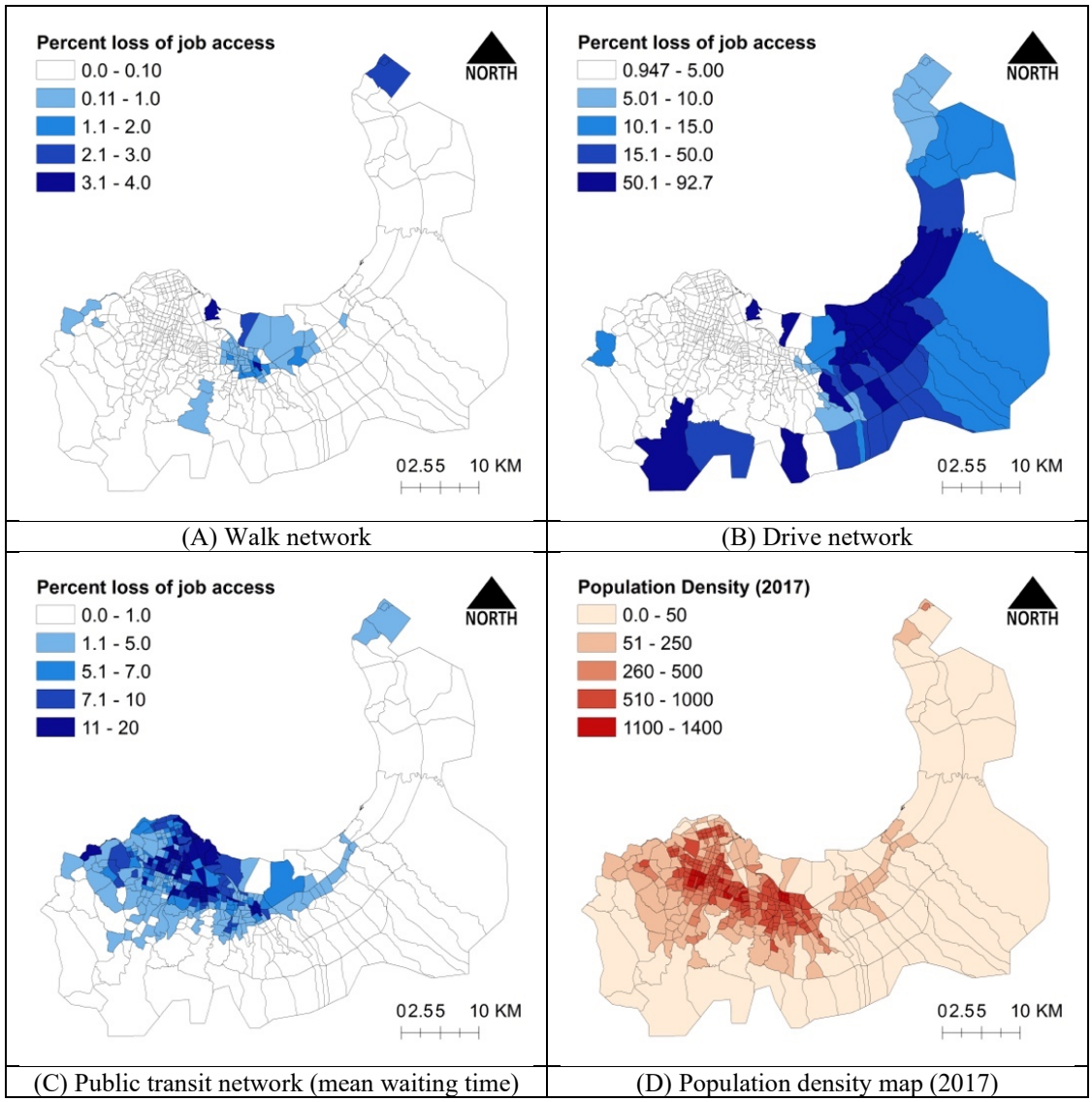

(A) Walk network | (B) Drive network

(C) Public transit network (mean waiting time) | (D) Population density map (2017)

Figure 14: Spatial distribution of percentage loss of job accessibility (due to10-year flood) for three different networks (panel A-C) and population density in 2017 (panel D)

Table 5: Comparison of one-hour job accessibility share under dry and wet conditions.

Network Type	Dry Condition Accessibility	Wet Condition Accessibility
Walk	9.1%	8.9%
Drive	84.7%	73.7%
Public Transit (mean waiting time)	20.4%	15.4%

4.3 Criticality

Transport criticality analysis generally refers to the rank-ordering process of transportation network components based on their contribution to certain aspects of overall network performance. The output of such analysis is useful in providing guidance to road administrations in their prioritization of maintenance and repair of roads (Jenelius et al., 2006). Currently, a variety of metrics have been shown to be useful in understanding network criticality (Jafino et al., 2020; Mattsson & Jenelius, 2015) including betweenness, change in average network efficiency, k-connectivity, minimum link cut centrality, etc. Table 6 provides a summary of network criticality metrics used in the existing literature. In this study, we choose betweenness centrality as a measure of road criticality due to its ability to provide a holistic view of the importance of road segments with respect to overall travel patterns.

Betweenness centrality is first defined by Freeman (1977, 1978) to understand node criticality/importance in social networks. It measures the number of times that a node or edge in a network acts as a 'bridge' in all-pairs shortest paths.[16] Usually, a 'bottleneck' node or edge in a transportation network will have higher betweenness than other peripheral nodes or edges. The conventional betweenness centrality derived from network theory is applied to the multi-modal network model in Kinshasa. We also adapted this metric to one that is able to capture network flows based on simulated travel trajectories leveraging the 8,866 trip OD information provided in the JICA commuters travel survey.

Table 6: Summary table of criticality metrics (adapted from Jafino et al. 2020).

No	Metric name	Description	Function	Scale
1	Change in weighted total travel cost	Increase in total travel cost (distance and traffic flow) among all origin-destination pairs due to disruptions on an element	Travel cost	Global
2	Change in expected user exposure	The average impact of disruptions experienced by all users in the transport system	Travel cost	Global
3	Change in worst-case user exposure	The maximum impact of disruptions among all users in the transport system	Travel cost	Global
4	Change in unweighted total travel cost	Increase in total travel cost (only distance) among all origin-destination pairs due to disruptions on an element	Travel cost	Global
5	Change in region-based unweighted total travel cost	Increase in total travel distance among all origin-destination pairs within a certain sub-area where the element is located due to disruptions on an element	Travel cost	Local
6	Change in weighted accessibility	Decrease in weighted (by transport demand/flow) accessibility due to disruptions of an element. The weight is determined by the socioeconomic activities	Accessibility	Global
7	Change in unweighted daily accessibility	Decrease in unweighted, topological-based accessibility due to disruptions of an element	Accessibility	Global
8	Traffic flow	Empirical traffic flow of the transport network	Travel cost	Local
9	Traffic density	Traffic volume over capacity. Normally used as an approximation of congestion	Travel cost	Local
10	Weighted betweenness centrality	The traffic flow among the economic centroids. The traffic flow is determined by the socioeconomic profiles	Travel cost	Local

[16]All-pairs shortest paths asks for the shortest path from every possible source to every possible destination.

11	Exposure to disaster	Overlay of natural disaster maps with the transport network. This is often used for disaster preparedness studies	Connectivity	Local
12	Nearby alternative elements	Number of other elements that are located within an x kilometer distance from an element.	Connectivity	Local
13	Unweighted betweenness centrality	Betweenness centrality calculated based on the shortest paths among the network nodes.	Travel cost	Local
14	Change in network average efficiency	Decrease in network efficiency due to disruptions of an element	Travel cost	Global
15	OD k-connectivity	Decrease in the number of distinct shortest paths among all origin-destination pair due to a disruption of an element	Connectivity	Global
16	Minimum link cut centrality	The frequency of a link,Äôs appearance in the cut sets of all pairs of economic centroids	Connectivity	Global
17	Unsatisfied demand	Amount of transport activity that cannot take place due to disruptions of an element	Connectivity	Global

Figure 15 shows the results of the betweenness centrality analysis based on the topological network of the combined four transportation layers: Taxi Jaune, Esprit de Vie, Transco Bus, and Esprit de Mort. The pedestrian network is left out, as the additional nodes and edges from the pedestrian network will skew the betweenness calculation output, thus obscuring the betweenness measures of the public transportation networks. In the figure, line segments shown in red are indicators of roads that have high betweenness from a topological perspective.[17] Roads with relatively high betweenness centrality include the N1 expressway, Avenue Sergent Moke, Avenue O.U.A., Rte de Matadi, and Avenue de l'Université. It should be noted that this calculation method makes assumptions about the travel patterns in the transportation network which introduces errors in the measurement of critical links/road segments in reality. For example, it is possible that a road segment with high betweenness centrality connects regions with low population density. This measure fails to take into consideration the usage of road segments in reality. Therefore, in addition we adopted another adapted calculation method which is based on travel paths simulations using OD pairs from the JICA travel survey.

Figure 16 shows the results from the adapted betweenness centrality calculation. The main difference between this adapted approach and the conventional one (Figure 15) is the way travel paths are calculated and accounted for. The conventional approach calculates shortest paths between every possible pair of nodes within the network whereas the adapted approach simulates the travel trajectories based on the multimodal transportation model and accounts for public transport waiting times, road speed limits, and designated origin and destination pairs acquired from the JICA commuter travel survey. This adapted approach is able to reflect the actual travel patterns within the network and identify critical links/segments which are most commonly used in reality. Results show that Avenue Du 24 Novembre, east-west sections of the N1 expressway (including Boulevard Triomphal, Boulevard Sendwe, Boulevard Lumumba) have high betweenness centrality. This means that many people rely on these roads for daily commute to work. If there are disruptions along these road segments due to floods or traffic accidents then many commuters will likely experience higher levels of delay due to vehicle speed reduction, congestion, rerouting, etc.

[17] The conventional betweenness measure focuses on the topology of the network itself and does not account for travel volume and patterns in the network.

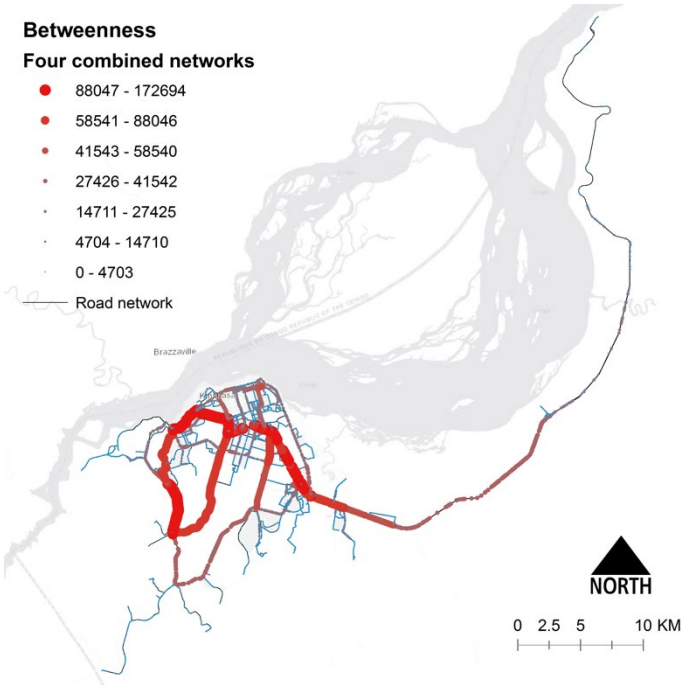

Figure 15: Betweenness centrality analysis on four combined public transportation layers.

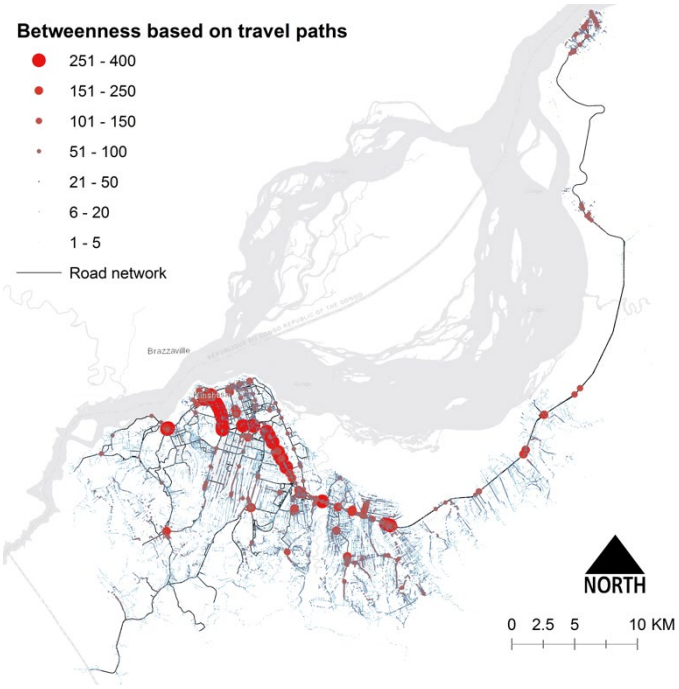

Figure 16: Betweenness centrality analysis based on travel paths from the JICA survey.

4.4 Economic Cost

The existing literature identifies two main types of impacts due to flooding on transportation networks and their associated costs: 1) tangible and intangible impacts (Hammond et al., 2015), 2) direct and indirect impacts (Messner, 2007). In general, tangible impact are those that can be readily quantified in monetary terms (D. I. Smith, 1999) including physical destruction of transportation infrastructures such as roads and bridges. In contrast, intangible impacts, such as negative disruptions to commuters' travel routes, are difficult to quantify. The second typology differentiates between direct and indirect damages where direct damage is defined as any loss that is caused by the immediate physical contact of floodwater with travelers and infrastructure property within flooded areas. Indirect damages are induced by the direct impacts and may occur – in space or time – beyond the immediate limits of the flood event (Hammond et al., 2015). The cost associated with these often includes additional costs incurred by diverting vehicles and trains in the entire transportation system, also known as consumer surplus (Nicholson & Du, 1997). Jonkman et al. (2008) integrated these two typologies and demonstrated that the impact and associated costs of flooding have multiple dimensions.

Among multiple dimensions of flood disruption on transport, travel time delay plays a major role in disruption costs calculation (Bivina et al., 2016). However, the question of how to value transport times is a challenging task that is the subject of numerous scientific papers and reports (Boiteux & Baumstarck, 2001; Litman, 2008; Mackie et al., 2003; Oort, 1969; Small et al., 2005). Past studies focus mainly on the topic of how to quantify the benefits of transport investments, which accrue in the form of travel time savings. Yet, there is no consensus, as estimates range from 25% (Litman, 2008) to close to 180% of an hourly wage with large heterogeneities depending on the traveler (Small et al., 2005). In this study, we provide a baseline estimation for travel time delay cost (calculated as a function of travel time delay and commuters' hourly income) as a lower bound for total economic cost due to flood disruption on road transportation networks.

This does not include other considerations such as production losses due to supply chain disruptions, or welfare implications of lost access to critical services and supplies.

To calculate the baseline travel delay cost, we first estimated the travel time for each commuter trip (8,866 total) under five flood scenarios using the walking, the drive and the public transit networks based on travel mode information reported in the JICA survey. Next, we calculated travel delay for each flood scenario by subtracting the travel time under dry condition from the estimations. This result was then combined with the personal monthly income information provided in the JICA survey. For each OD trip, we multiplied the delay in travel time due to flooding by the income per unit of time assuming that each worker works eight hours a day, five days a week, and on average 22 days a month. The corresponding output was then doubled to account for return trips from work. To adjust for the difference between sample size and survey population, the cost was multiplied by respective weighting factors for each trip. This same process was repeated for five flood return periods namely: 10-year, 50-year, 100-year, 500-year and 1000-year and the economic cost for all 8,866 trips were later aggregated to the TAZ level. Table 7 shows the number of commuters' trips affected by five flood scenarios under different delay thresholds. Figure 17 illustrates maps of the averaged economic cost due to travel delay for each TAZ under all flood scenarios. We observe that areas towards the center of Kinshasa city experience relatively higher cost than peripheral suburbs in the south-east and north-east with the exception of the smaller TAZs situated in the heart of the city. It should be noted that the averaged cost aggregation at the TAZ level is more representative in the central regions of the city. Due to the uneven spatial distribution of sampling locations, the peripheral TAZs only contain a few sampling points. For example, the Kinsielele region towards the south of the city shows up with relatively high travel delay costs under all flood scenarios yet there are only 11 sampling points in this particular TAZ.

Figure 18 shows two sets of grouped boxplots of estimated travel time delay in minutes and corresponding economic loss for different levels of personal income under five flood scenarios. In general, floods with longer return periods (more extreme) on average induce longer travel delays and more economic cost compared with those of shorter return periods. When it comes to the variation or uncertainty of flood impacts, the 100-year and 500-year floods are relatively higher than floods of other return periods. Specifically, the 100-year flood's impact on commuters' travel delays has the highest variation/uncertainty and the 500-year flood is the highest in terms of economic cost variation/uncertainty. When we examine these two types of impact: travel delay and economic cost by different income groups, it is clear that commuters with medium income levels (monthly salary from $100 to $1,000) experience relatively higher travel delays than low income (monthly salary below $100) commuters and high income (monthly salary greater than $3,000) commuters. It should be noted that the lower-income groups have more extreme estimates (over one hour) in travel delays which suggest the existence of highly disadvantaged commuter groups who are heavily impacted by flood disruptions on road networks.

Table 7: Number of commuter trips affected (8866 total) by delay thresholds.

Flood return period	>5 min delay	>10 min delay	>30 min delay	>1 hour delay	>2 hour delay	Number of failed trips
10-year flood	7520	6491	4261	2418	342	679
50-year flood	7007	6047	4085	2810	1049	1217
100-year flood	6779	5842	4032	3027	1821	1453
500-year flood	5940	5047	3408	2590	1822	2329
1000-year flood	5344	4475	2878	2108	1477	2924

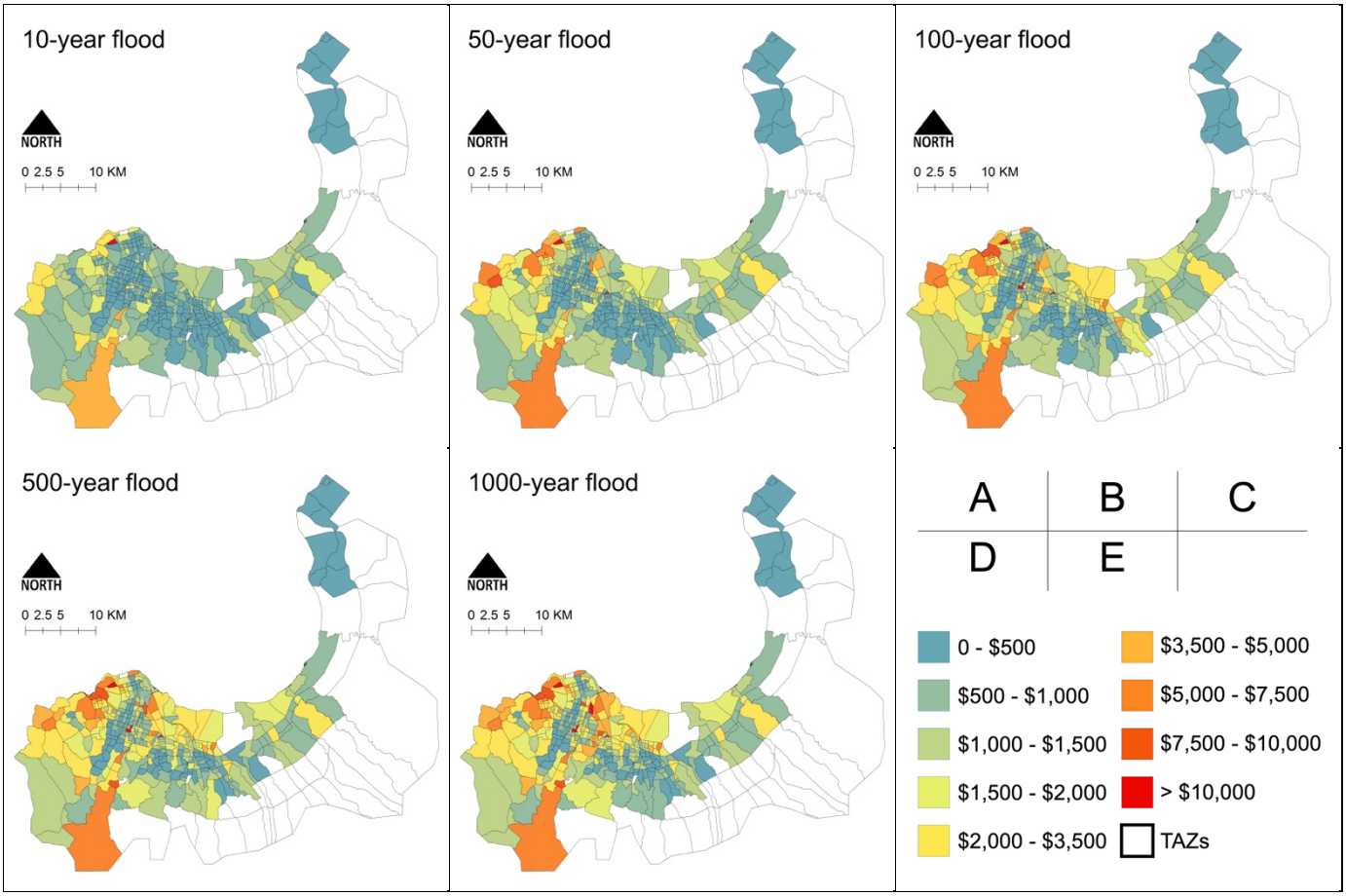

Figure 17: Daily total cost from from flood-related commuting delays at the TAZ level under five flood scenarios.

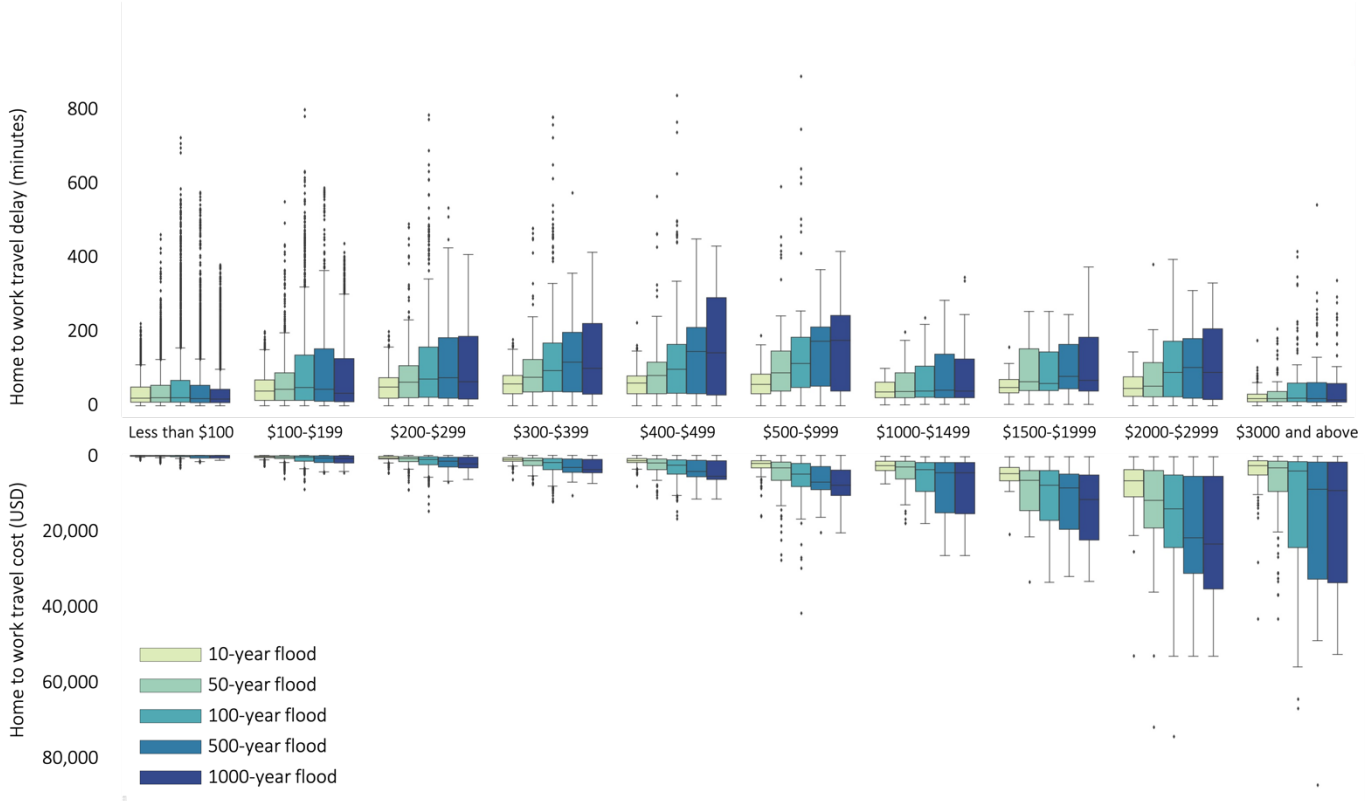

Figure 18: Histogram of estimated economic loss by income level under five flood scenarios.

In sum, the total weighted daily travel delay costs[18] due to 10-year, 50-year, 100-year, 500-year and 1000-year floods are $5,367,000, $8,642,000, $11,628,000, $13,304,000 and $14,374,000 respectively. When taking flood occurrence probability (i.e. 1in 10, 50, 100, 500 and 1000 years) into consideration, the average daily transport disruption cost weighted by occurrence probability is $1,166,000. If we assume that on average there are 28 days of flood disruptions on the Kinshasa transportation network then the annualized amount lost to floods is $32,648,000. It should be underlined that these amounts, because they only consider time lost for commuting purposes and not direct damages or other indirect costs such as disrupted supply chains, constitute a conservative evaluation of the costs of floods in Kinshasa.

5 Conclusion and Discussion

In Kinshasa, DRC, the combination of pluvial and fluvial floods of multiple return periods impacts all transportation modes and causes a reduction in vehicle speeds, road closures, lengthened daily commute patterns, reduced job accessibility and economic costs due to travel delay. Under wet conditions, the headways for transit modes such as Esprit de Mort increase by 42% from 31 to 44 minutes on average. Flood water accumulation on road surfaces that exceeds 0.2 meters in depth will cause road closures and blockages. Consequently, commuters' daily trips to and from work need to be rerouted or canceled resulting in pronounced delays in travel time and associated economic costs. Based on our estimation, the total economic cost with respect to daily commuters' travel delay is $5,367,000 under the 10-year flood scenario. Combined with simulated outputs from multiple flood return periods, the daily weighted average of travel delay cost caused by flood occurrence probability is $1,166,000. It should be noted that this estimation provides a lower bound to the total economic loss due to such type of flooding because it does not account for direct damages to transport infrastructure and for other indirect damages such as production losses due to supply chain disruptions, or welfare implications of lost accessibility to critical services and supplies.

Several other findings and conclusions emerge from our analysis. First, accessibility to jobs decreases under wet road conditions. On average, the share of jobs that can be reached within one hour will decrease by 0.1% for the walking network, 10.9% for the driving network, and 5.0% for the public transit network. Combined with visualizations of the spatial distribution of loss of job accessibility at TAZ level for three networks (Figure 14), the government as well as planning and design agencies can target specific areas and regions for road fortification and better integration of multiple transport modes to minimize the loss. Second, we observe heterogeneity in travel time impact pattern from floods from both spatial and socio-economical perspectives. In some areas within the Kinshasa city (e.g. Kimbanseke), the income level of its residents is relatively low whereas the travel delay they experience during a 10-year flood event (based on our simulation) is relatively high. The exact opposite pattern can be observed in areas such as Centre Ville, Lingwala, Barumbu, etc. This pattern raises socio-spatial equity issues which are important for public policy considerations. Similar disparities can also be observed for other flood return periods with more extreme values due to travel delays for lower-income groups. These results provide valuable guidelines for planning efforts to target disadvantaged groups and communities for physical and financial aid support. Third, our modified road segment criticality analysis sheds light on the prioritization of road interventions to increase transportation resilience to floods. City officials and transportation planners in Kinshasa aiming to climate-proof the city's transport network face difficult choices in where to start. These results provide some

[18] The total cost is an estimation of the economic cost to commuters, associated with one day of flooded road conditions in the 10-year flood scenario.

guidance as to which road segments to invest first based on their importance in maintaining decent travel times for many commuters under wet conditions.

Finally, we hope to point out that given climatic uncertainties in the future, the frequency and magnitude of floods in Kinshasa and other regions around the world will likely increase. The 10-year flood scenario has the lowest exposure level among all five flood return periods that we examined in this study. As climate change impacts unfold over time, the potential impact of floods on transportation is likely to increase dramatically. It is possible to imagine that the economic cost we report for the current 50-year flood event, for example, will occur more frequently in the future, thereby increasing the returns from resilient transport infrastructure planning and design in Kinshasa.

A limited number of uncertainty areas deserve some discussion. First, because of the difficulty of surveying the entire public transport network during the narrow window when floods are still affecting travel conditions, only a share (approximately 25%) of routes were mapped under wet conditions. While we implemented strategies to overcome this data incompleteness and were able to draw valuable and reasonable insights from the sampled data, future studies could provide a more complete picture of public transport during heavy rain episodes in developing country cities and could help establish causal chains between floods, vehicle frequencies, rerouting and decreased travel speeds more clearly. Ongoing work on the city of Kigali, Rwanda, which has a smaller population, urban footprint and public transport network, will include a survey of the entire transit system in both dry and wet conditions, and will provide a more complete and precise picture of public transport disruptions from floods. Second, in our study, we used mosaics of the maximum value of each raster pixel from fluvial and pluvial flood map products to approximate flood depth and extent induced by the combination of both types of floods. Although this provides a useful estimate that captures the extremes of both types of floods, such operation lacks considerations of the hydrodynamics of flood processes and may introduce error and uncertainties in flood depth and extent estimations.

6 References

Bernhofen, M. V., Whyman, C., Trigg, M. A., Sleigh, P. A., Smith, A. M., Sampson, C. C., Yamazaki, D., Ward, P. J., Rudari, R., Pappenberger, F., Dottori, F., Salamon, P., & Winsemius, H. C. (2018). A first collective validation of global fluvial flood models for major floods in Nigeria and Mozambique. *Environmental Research Letters*, *13*(10), 104007. https://doi.org/10.1088/1748-9326/aae014

Bivina, G. R., Landge, V., & Kumar, V. S. S. (2016). Socio Economic Valuation of Traffic Delays. *Transportation Research Procedia*, *17*, 513–520. https://doi.org/10.1016/j.trpro.2016.11.104

Boeing, G. (2017). OSMnx: New methods for acquiring, constructing, analyzing, and visualizing complex street networks. *Computers, Environment and Urban Systems*, *65*, 126–139. https://doi.org/10.1016/j.compenvurbsys.2017.05.004

Boiteux, M., & Baumstarck, L. (2001). *Transports: Choix des investissements et coût des nuisances*. Commissariat général du plan.

Chen, Z., & Wang, Y. (2019). Impacts of severe weather events on high-speed rail and aviation delays. *Transportation Research Part D: Transport and Environment*, *69*, 168–183. https://doi.org/10.1016/j.trd.2019.01.030

DfT. (2014). *Transport resilience review: A review of the resilience of the transport network to extreme weather events*. Stationery Office.

Efron, B., & Tibshirani, R. J. (1993). *An Introduction to the Bootstrap* (1st Edition). Chapman and Hall/CRC.

Freeman, L. C. (1977). A Set of Measures of Centrality Based on Betweenness. *Sociometry*, *40*(1), 35–41. JSTOR. https://doi.org/10.2307/3033543

Freeman, L. C. (1978). Centrality in social networks conceptual clarification. *Social Networks*, *1*(3), 215–239. https://doi.org/10.1016/0378-8733(78)90021-7

GTFS. (2020). *General Transit Feed Specification*. https://gtfs.org/

Hall, J. W., Dawson, R. J., Sayers, P. B., Rosu, C., Chatterton, J. B., & Deakin, R. (2003). A methodology for national-scale flood risk assessment. *Proceedings of the Institution of Civil Engineers - Water and Maritime Engineering*, *156*(3), 235–247. https://doi.org/10.1680/wame.2003.156.3.235

Hammond, M. J., Chen, A. S., Djordjević, S., Butler, D., & Mark, O. (2015). Urban flood impact assessment: A state-of-the-art review. *Urban Water Journal*, *12*(1), 14–29. https://doi.org/10.1080/1573062X.2013.857421

International Federation of Red Cross and Red Crescent Societies. (2018). *Emergency Plan of Action (EPoA) Democratic Republic of the Congo: Floods in Kinshasa*. https://reliefweb.int/report/democratic-republic-congo/democratic-republic-congo-floods-kinshasa-emergency-plan-action

IPCC. (2014). *IPCC 5th Assessment Synthesis Report*. IPCC 5th Assessment Synthesis Report. http://ar5-syr.ipcc.ch/topic_futurechanges.php

Jafino, B. A., Kwakkel, J., & Verbraeck, A. (2020). Transport network criticality metrics: A comparative analysis and a guideline for selection. *Transport Reviews*, *40*(2), 241–264. https://doi.org/10.1080/01441647.2019.1703843

Jenelius, E., Petersen, T., & Mattsson, L.-G. (2006). Importance and exposure in road network vulnerability analysis. *Transportation Research Part A: Policy and Practice*, *40*(7), 537–560. https://doi.org/10.1016/j.tra.2005.11.003

JICA. (2018). *Project Research on "Transportation Survey and Travel Demand Forecast in Developing Countries*. https://openjicareport.jica.go.jp/pdf/12339883.pdf

Jonkman, S. N., Bočkarjova, M., Kok, M., & Bernardini, P. (2008). Integrated hydrodynamic and economic modelling of flood damage in the Netherlands. *Ecological Economics*, *66*(1), 77–90. https://doi.org/10.1016/j.ecolecon.2007.12.022

Kasmalkar, I. G., Serafin, K. A., Miao, Y., Bick, I. A., Ortolano, L., Ouyang, D., & Suckale, J. (2020). When floods hit the road: Resilience to flood-related traffic disruption in the San Francisco Bay Area and beyond. *Science Advances*, *6*(32), eaba2423. https://doi.org/10.1126/sciadv.aba2423

Kim, B., Shin, S. C., & Kim, D. Y. (2018). Scenario-Based Economic Impact Analysis for Bridge Closures Due to Flooding: A Case Study of North Gyeongsang Province, South Korea. *Water*, *10*(8), 981. https://doi.org/10.3390/w10080981

Kim, T. J., Ham, H., & Boyce, D. E. (2002). Economic impacts of transportation network changes: Implementation of a combined transportation network and input-output model*. *Papers in Regional Science*, *81*(2), 223–246. https://doi.org/10.1111/j.1435-5597.2002.tb01231.x

Kinshasa. (2020). In *Wikipedia*. https://en.wikipedia.org/w/index.php?title=Kinshasa&oldid=968392834

Krambeck, H., & Qu, L. (2015). Toward an Open Transit Service Data Standard in Developing Asian Countries. *Transportation Research Record*, *2538*(1), 30–36. https://doi.org/10.3141/2538-04

Litman, T. (2008). Valuing Transit Service Quality Improvements. *Journal of Public Transportation*, *11*(2), 43–63. https://doi.org/10.5038/2375-0901.11.2.3

Mackie, P. J., Wardman, M., Fowkes, A. S., Whelan, G., Nellthorp, J., & Bates, J. (2003). *Values of travel time savings UK*. Institute of Transport Studies.

Mao, L.-Z., Zhu, H.-G., & Duan, L.-R. (2012). *The Social Cost of Traffic Congestion and Countermeasures in Beijing*. 68–76. https://doi.org/10.1061/9780784412299.0010

Maruyama Rentschler, J. E., Braese, J. M., Jones, N., & Avner, P. (2019). *Three Feet Under: The Impact of Floods on Urban Jobs, Connectivity, and Infrastructure* (SSRN Scholarly Paper ID 3430508). Social Science Research Network. https://papers.ssrn.com/abstract=3430508

Mattsson, L.-G., & Jenelius, E. (2015). Vulnerability and resilience of transport systems − A discussion of recent research. *Transportation Research Part A: Policy and Practice*, *81*, 16–34. https://doi.org/10.1016/j.tra.2015.06.002

Messner, F. (2007). Evaluating flood damages: Guidance and recommendations on principles and methods. *T09-06-01*. https://repository.tudelft.nl/islandora/object/uuid%3A5602db10-274c-40da-953f-34475ded1755

Moovit. (2020). *Transco Bus routes, Bus times and schedule in Kinshasa*. https://moovitapp.com/index/en/public_transit-lines-Kinshasa-5983-1610334

Nicholson, A., & Du, Z.-P. (1997). Degradable transportation systems: An integrated equilibrium model. *Transportation Research Part B: Methodological*, *31*(3), 209–223. https://doi.org/10.1016/S0191-2615(96)00022-7

Okuyama, Y. (2007). Economic Modeling for Disaster Impact Analysis: Past, Present, and Future. *Economic Systems Research*, *19*(2), 115–124. https://doi.org/10.1080/09535310701328435

O′Loughlin, F. E., Neal, J., Schumann, G. J. P., Beighley, E., & Bates, P. D. (2020). A LISFLOOD-FP hydraulic model of the middle reach of the Congo. *Journal of Hydrology*, *580*, 124203. https://doi.org/10.1016/j.jhydrol.2019.124203

Oort, C. J. (1969). The Evaluation of Travelling Time. *Journal of Transport Economics and Policy*, *3*(3), 279–286. https://doi.org/10.2307/20052155

Perrine, K., Khani, A., & Ruiz-Juri, N. (2015). Map-Matching Algorithm for Applications in Multimodal Transportation Network Modeling. *Transportation Research Record*, *2537*(1), 62–70. https://doi.org/10.3141/2537-07

Pregnolato, M., Ford, A., Glenis, V., Wilkinson, S., & Dawson, R. (2017). Impact of Climate Change on Disruption to Urban Transport Networks from Pluvial Flooding. *Journal of Infrastructure Systems*, *23*(4), 04017015. https://doi.org/10.1061/(ASCE)IS.1943-555X.0000372

Pregnolato, M., Ford, A., Wilkinson, S. M., & Dawson, R. J. (2017). The impact of flooding on road transport: A depth-disruption function. *Transportation Research Part D: Transport and Environment*, *55*, 67–81. https://doi.org/10.1016/j.trd.2017.06.020

Schreider, S. Yu., Smith, D. I., & Jakeman, A. J. (2000). Climate Change Impacts on Urban Flooding. *Climatic Change*, *47*(1), 91–115. https://doi.org/10.1023/A:1005621523177

Singh, P., Sinha, V. S. P., Vijhani, A., & Pahuja, N. (2018). Vulnerability assessment of urban road network from urban flood. *International Journal of Disaster Risk Reduction*, *28*, 237–250. https://doi.org/10.1016/j.ijdrr.2018.03.017

Small, K. A., Winston, C., & Yan, J. (2005). Uncovering the Distribution of Motorists′ Preferences for Travel Time and Reliability. *Econometrica*, *73*(4), 1367–1382. https://doi.org/10.1111/j.1468-0262.2005.00619.x

Smith, A., Sampson, C., & Bates, P. (2015). Regional flood frequency analysis at the global scale. *Water Resources Research*, *51*(1), 539–553. https://doi.org/10.1002/2014WR015814

Smith, D. I. (1999). Floods: Physical processes and human impacts by K. Smith and R. Ward, John Wiley, Chichester 1998. No. of pages: 382. *Earth Surface Processes and Landforms*, *24*(13), 1261–1261. https://doi.org/10.1002/(SICI)1096-9837(199912)24:13<1261::AID-ESP22>3.0.CO;2-#

Stewart, A. (2006). Assessing the Economic Impacts of Transportation Improvement Projects. *Theses and Dissertations*. https://scholarsarchive.byu.edu/etd/406

Tatano, H., & Tsuchiya, S. (2008). A framework for economic loss estimation due to seismic transportation network disruption: A spatial computable general equilibrium approach. *Natural Hazards*, *44*(2), 253–265. https://doi.org/10.1007/s11069-007-9151-0

Tshimanga, R. M., Tshitenge, J. M., Kabuya, P., Alsdorf, D., Mahe, G., Kibukusa, G., & Lukanda, V. (2016). Chapter 4—A Regional Perceptive of Flood Forecasting and Disaster Management Systems for the Congo River Basin. In T. E. Adams & T. C. Pagano (Eds.), *Flood Forecasting* (pp. 87–124). Academic Press. https://doi.org/10.1016/B978-0-12-801884-2.00004-9

Wong, J. C. (2013). *Use of the general transit feed specification (GTFS) in transit performance measurement* [Thesis, Georgia Institute of Technology]. https://smartech.gatech.edu/handle/1853/50341

Wood, E. F., Roundy, J. K., Troy, T. J., Beek, L. P. H. van, Bierkens, M. F. P., Blyth, E., Roo, A. de, Döll, P., Ek, M., Famiglietti, J., Gochis, D., Giesen, N. van de, Houser, P., Jaffé, P. R., Kollet, S., Lehner, B., Lettenmaier, D. P., Peters-Lidard, C., Sivapalan, M., … Whitehead, P. (2011). Hyperresolution global land surface modeling: Meeting a grand challenge for monitoring Earth′s terrestrial water. *Water Resources Research*, *47*(5). https://doi.org/10.1029/2010WR010090

World Bank. (2020). *World Bank Open Data | Data*. https://data.worldbank.org/

Yin, J., Yu, D., Yin, Z., Liu, M., & He, Q. (2016). Evaluating the impact and risk of pluvial flash flood on intra-urban road network: A case study in the city center of Shanghai, China. *Journal of Hydrology*, *537*, 138–145. https://doi.org/10.1016/j.jhydrol.2016.03.037

7 Appendix A

Estimating work locations for missing records

In this study, the commuter travel survey from JICA is used to provide information on daily worker travel patterns in Kinshasa. Specifically, we use the trip origin and destination locations provided in the survey as input for travel simulation. However, approximately 40% of the records provided are missing detailed information on the workplace latitudes and longitudes. This creates a major barrier in our analysis workflow, so we decided to use a statistical approach to predict/estimate the workplace latitudes and longitudes. The specific method we used is K-nearest neighbor (KNN).

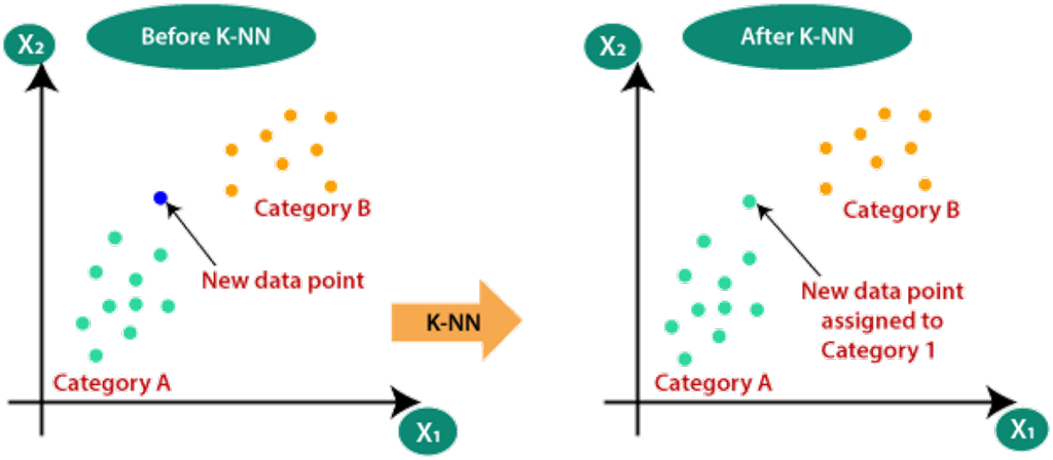

Figure 19: Conceptual illustration of how K-nearest neighbor works. Source: https://www.javatpoint.com/k-nearest-neighbor-algorithm-for-machine-learning.

KNN is one of the simplest Machine Learning (ML) algorithms based on supervised Learning technique. It assumes similarity between the unknown data and available data and makes predictions on the unknown data base on its similarity with the available data (Figure 19). In our analysis, we use the survey records that both household and workplace latitudes and longitudes are available as the training data pool and evaluate the similarity between unknown records with existing records using seven features: Household longitude, Household latitude, Household TAZ, Household income, Personal income, Workplace type, and Employment status. The training error is zero meters and the testing error is 8,000 meters on average and eight meters at minimum.